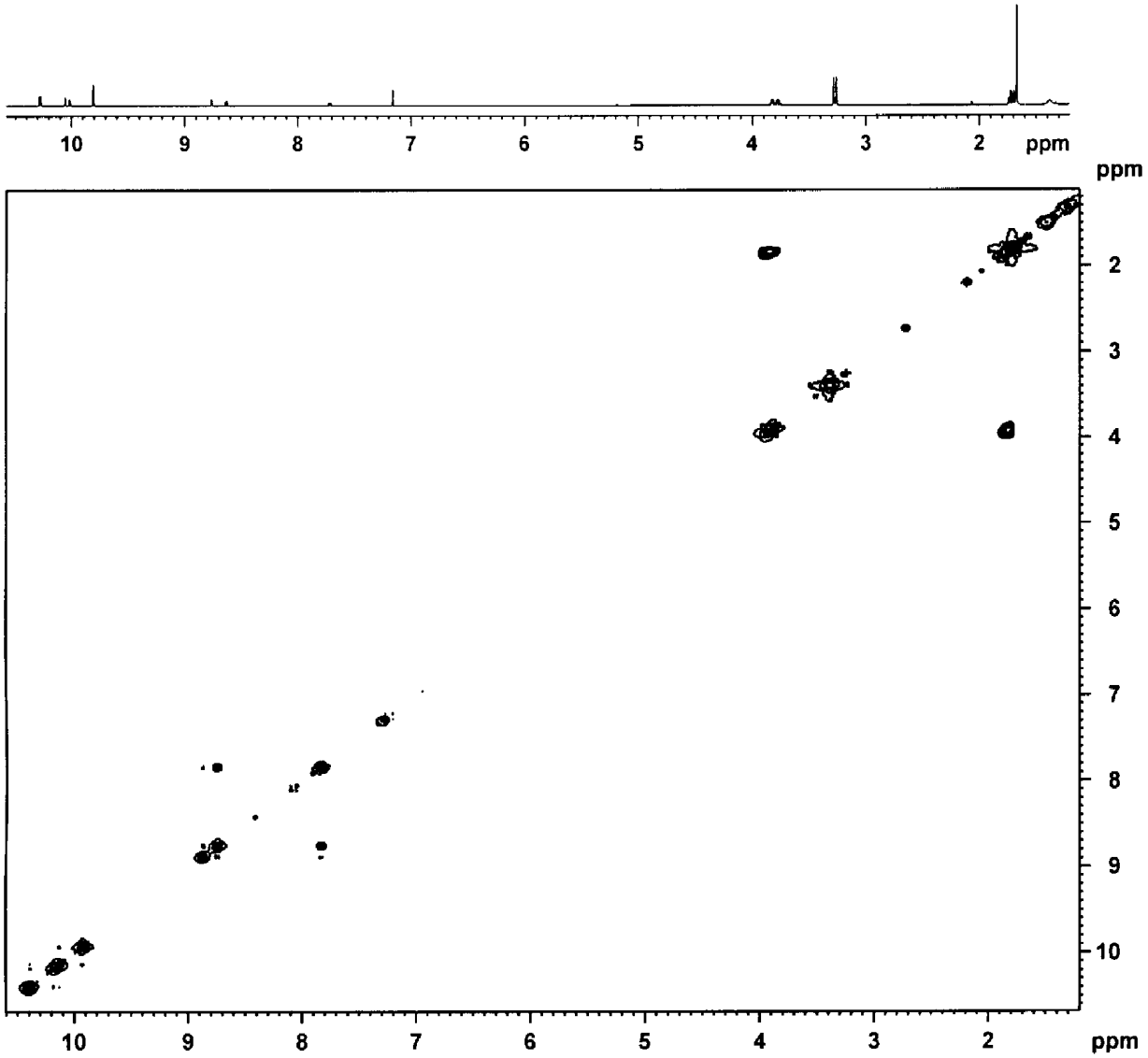

Figure S96. ^{1}H-^{1}H COSY NMR spectrum of *tert*-butyl benzoselenacarbaporphyrin **15c** in $CDCl_3$.

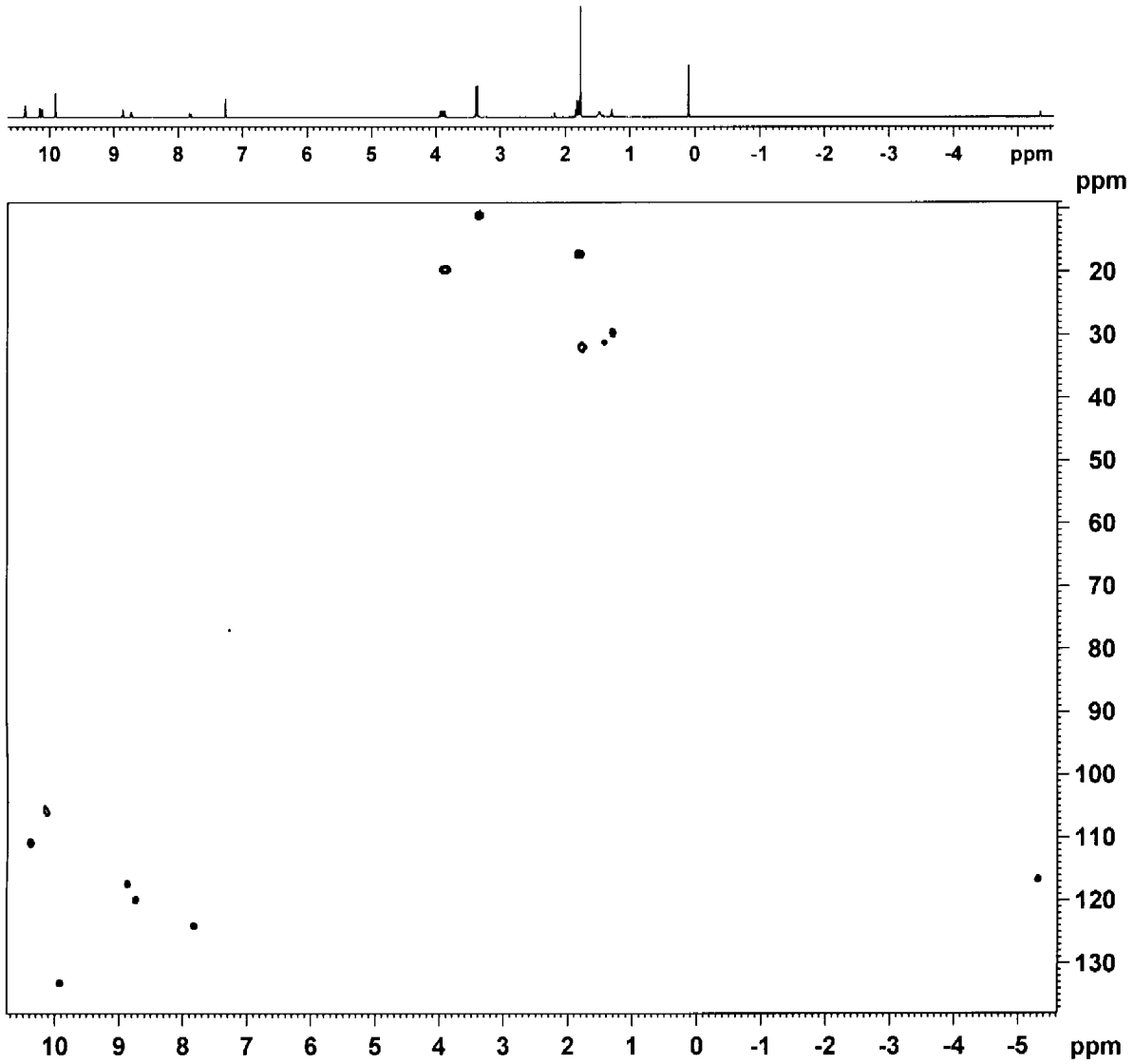

Figure S97. HSQC NMR spectrum of *tert*-butyl benzoselenacarbaporphyrin **15c** in $CDCl_3$.

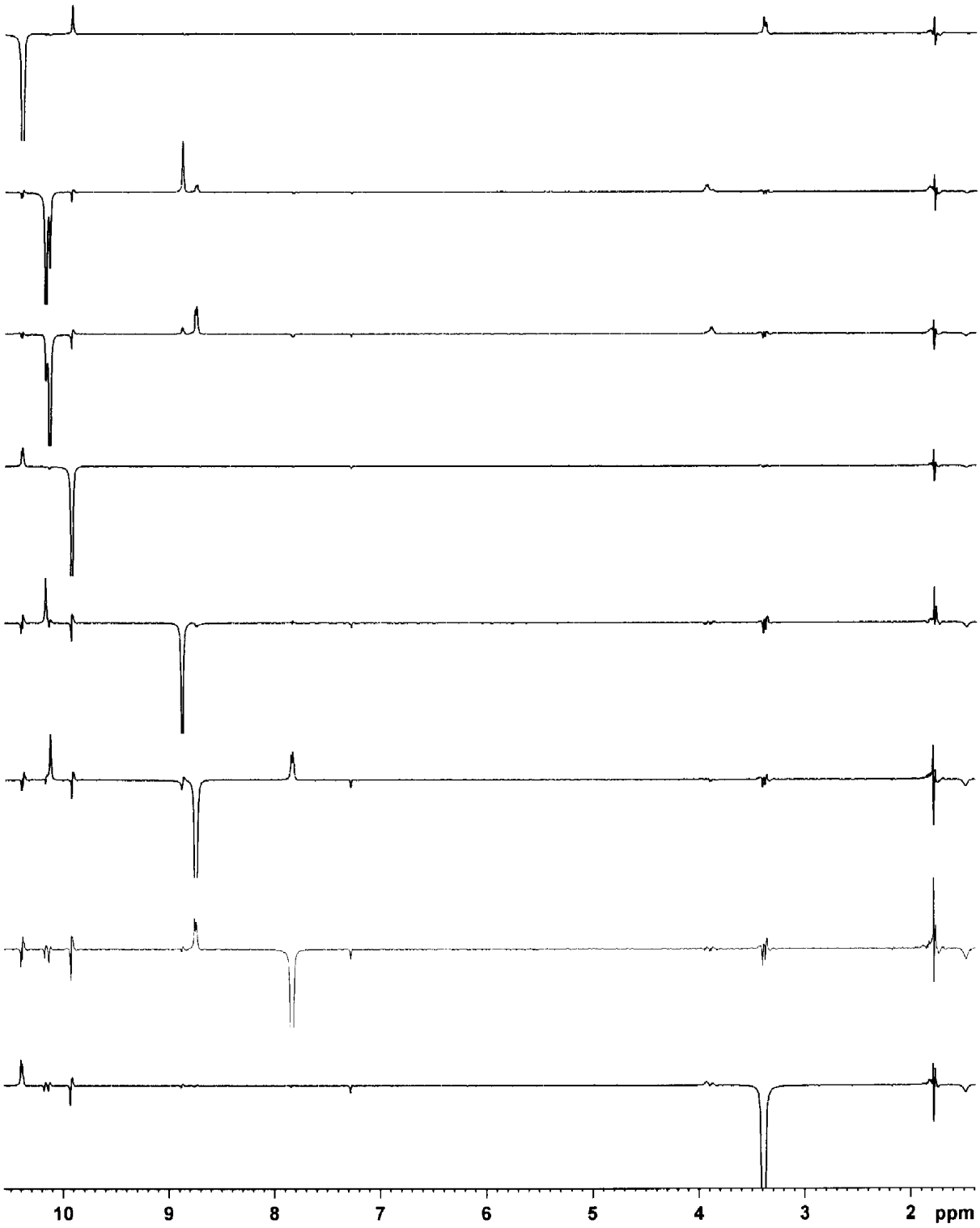

Figure S98. Selected nOe difference proton NMR spectra of **15c** in $CDCl_3$.

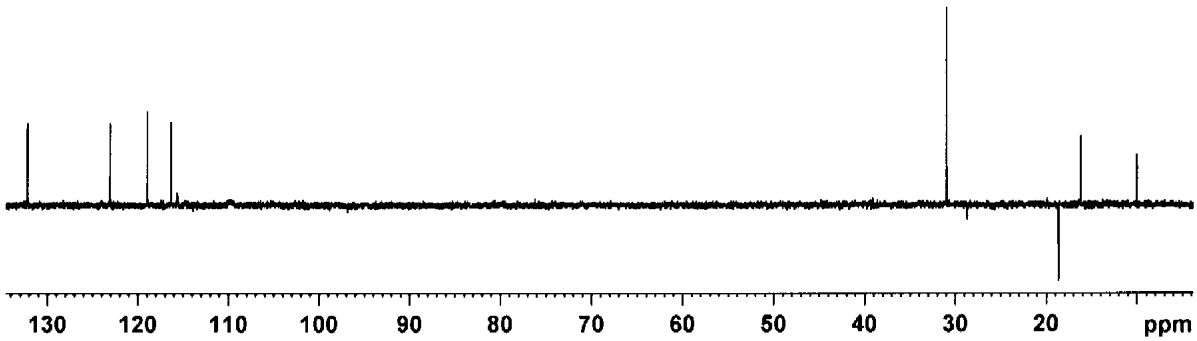

Figure S99. DEPT-135 NMR spectrum of **15c** in $CDCl_3$.

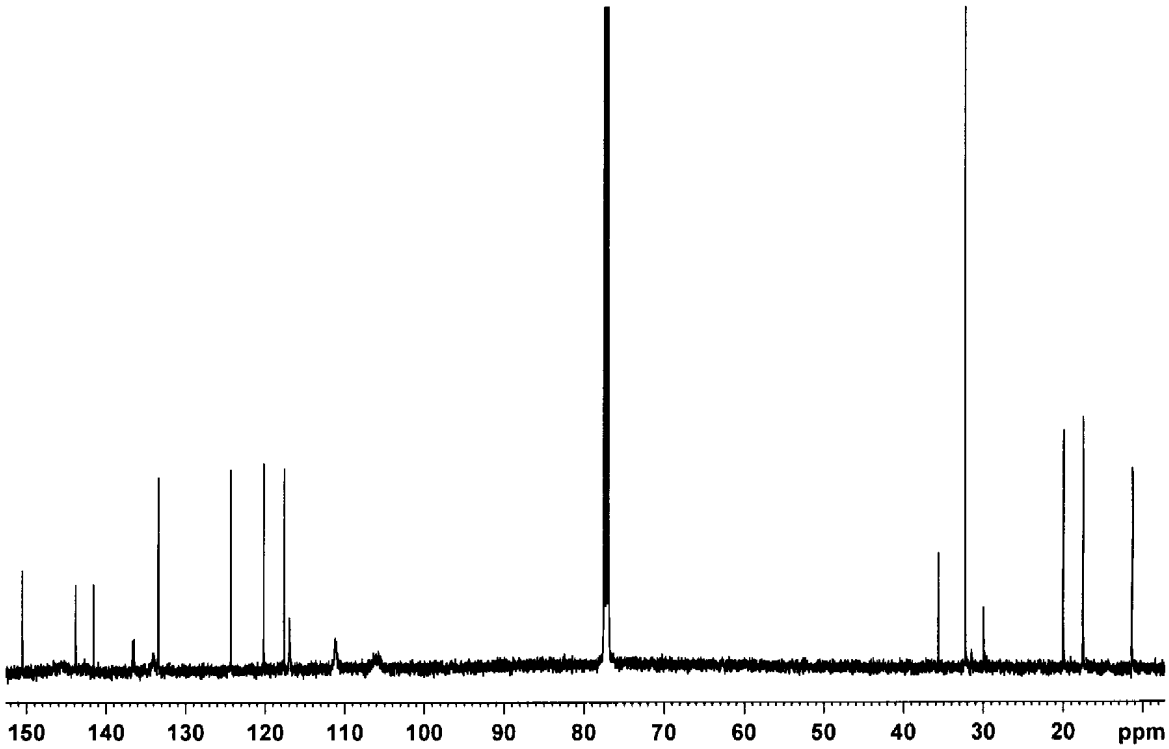

Figure S100. 125 MHz carbon-13 NMR spectrum of **15c** in $CDCl_3$ at 50 ^{o}C.

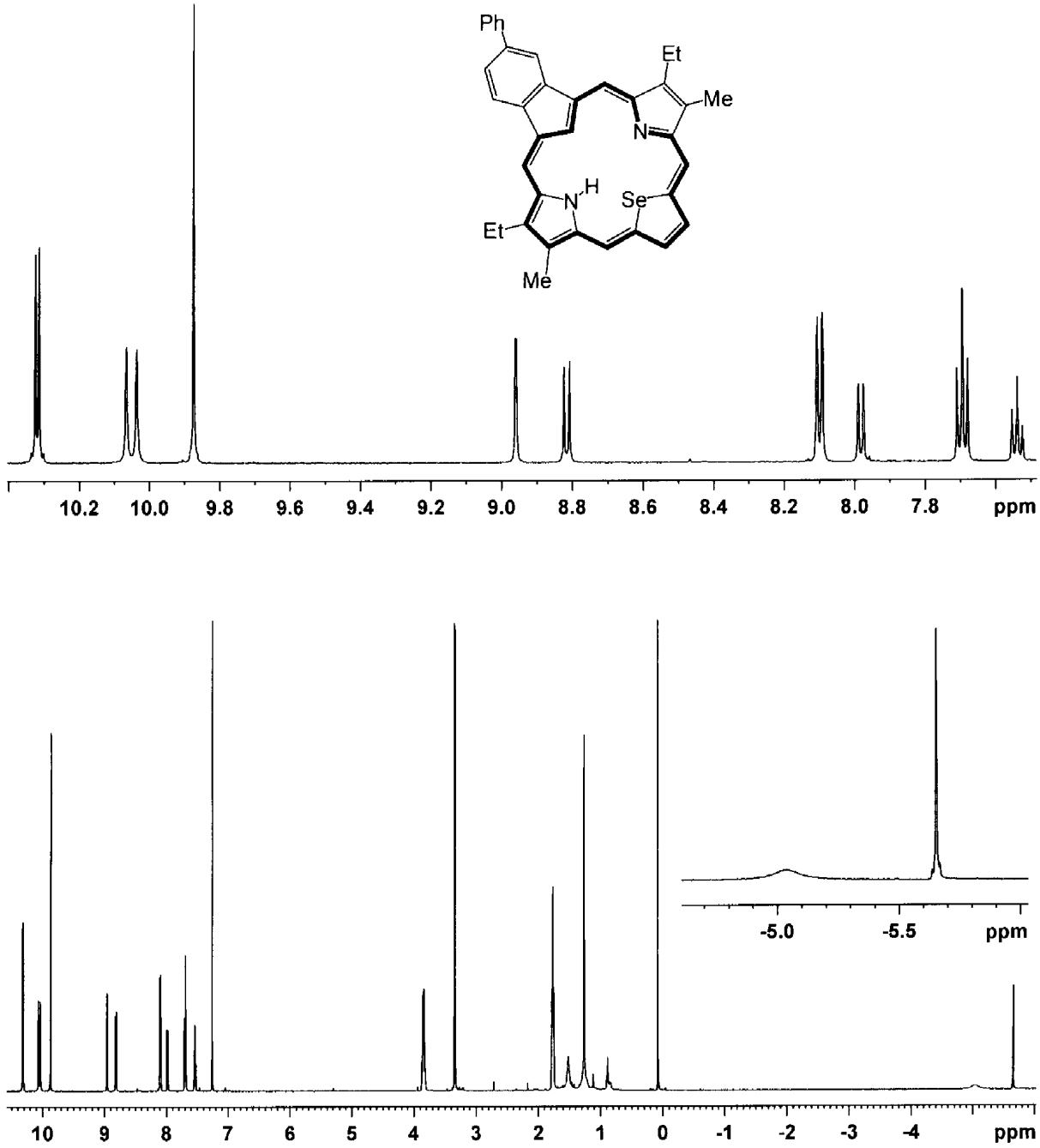

Figure S101. 500 MHz proton NMR spectrum of phenyl benzoselenacarbaporphyrin **15d** in $CDCl_3$.

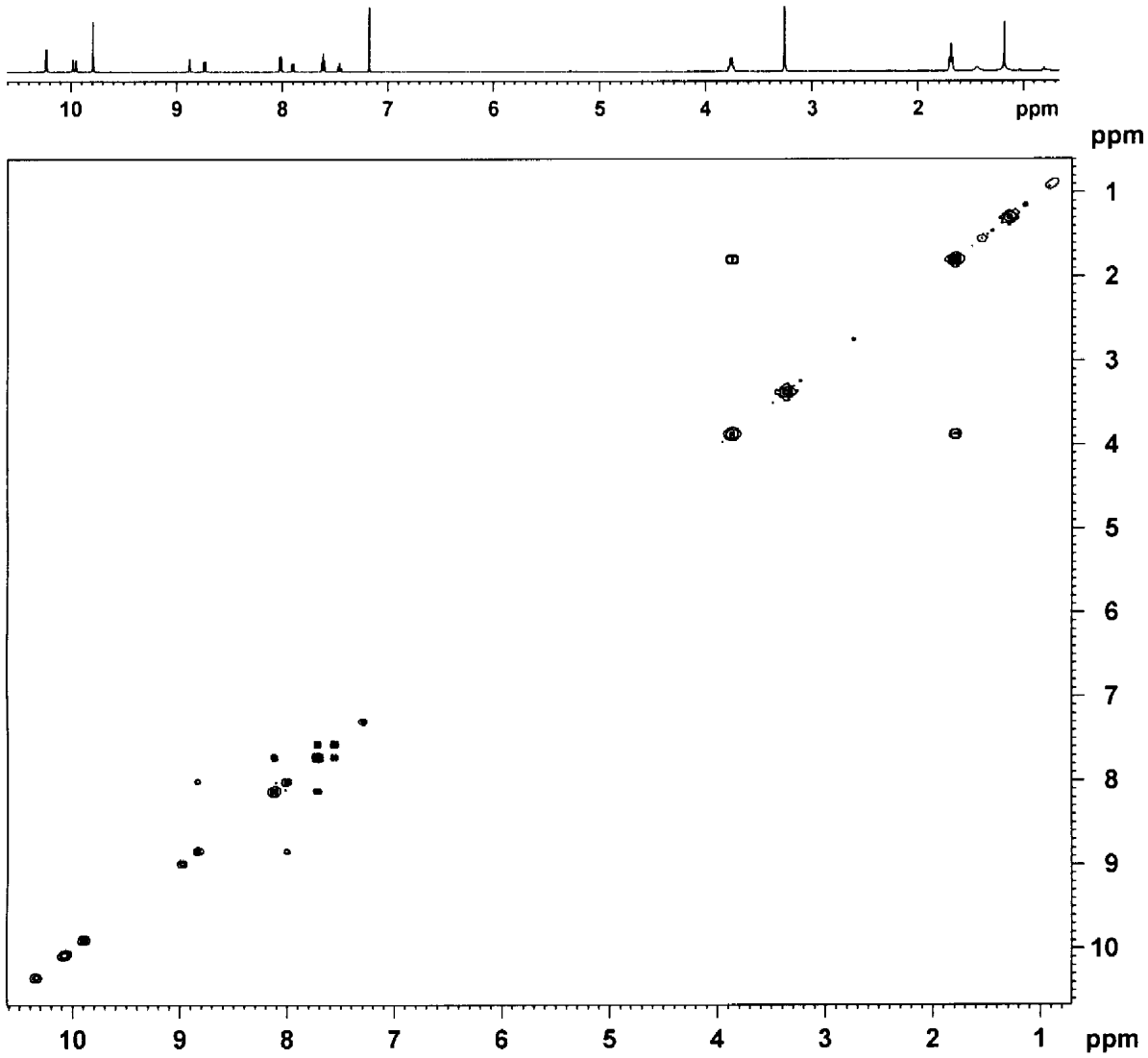

Figure S102. ^{1}H-^{1}H COSY NMR spectrum of phenyl benzoselenacarbaporphyrin **15d** in $CDCl_3$.

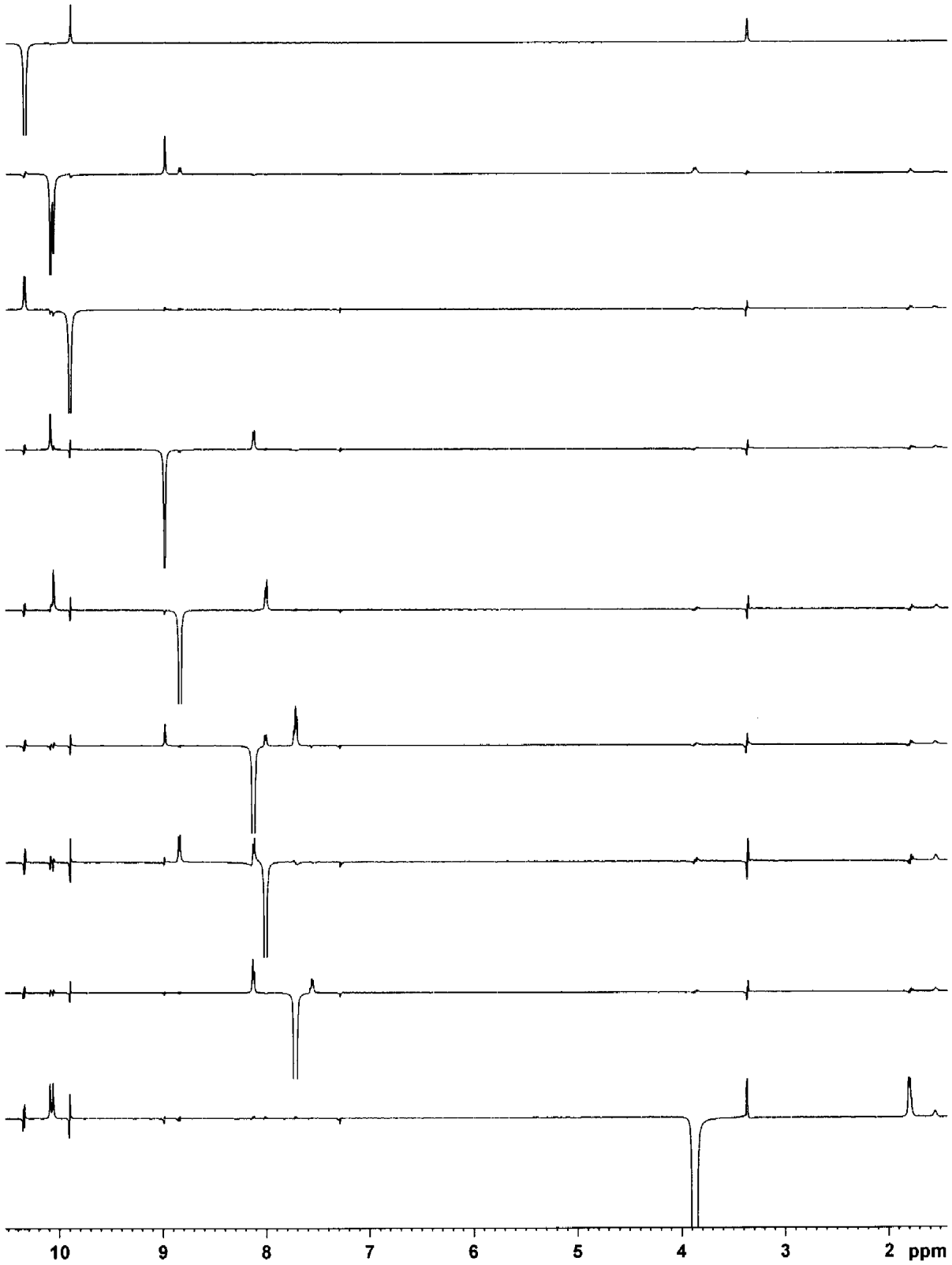

Figure S103. Selected nOe difference proton NMR spectra of **15d** in $CDCl_3$.

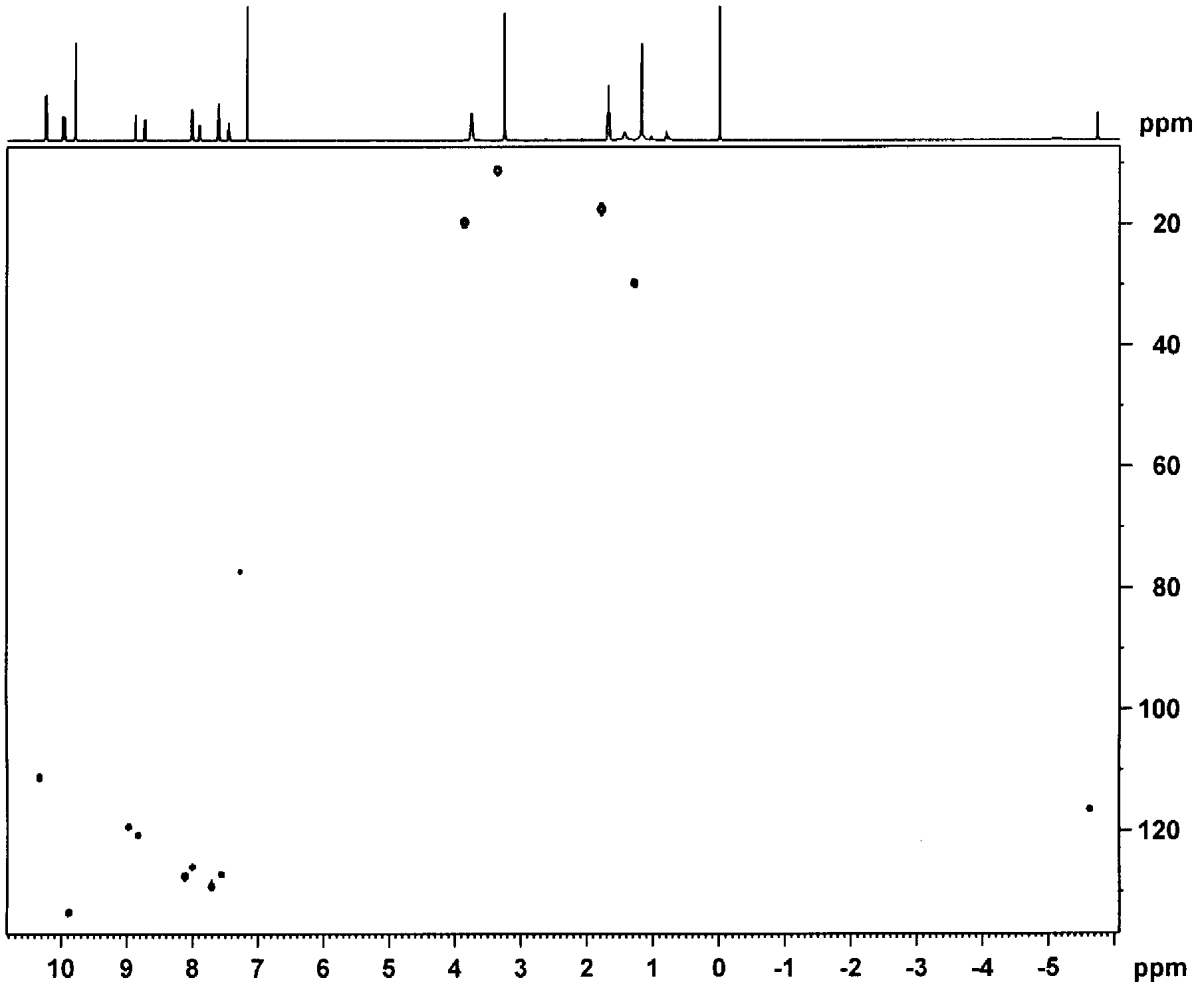

Figure S104. HSQC NMR spectrum of phenyl benzoselenacarbaporphyrin **15d** in $CDCl_3$.

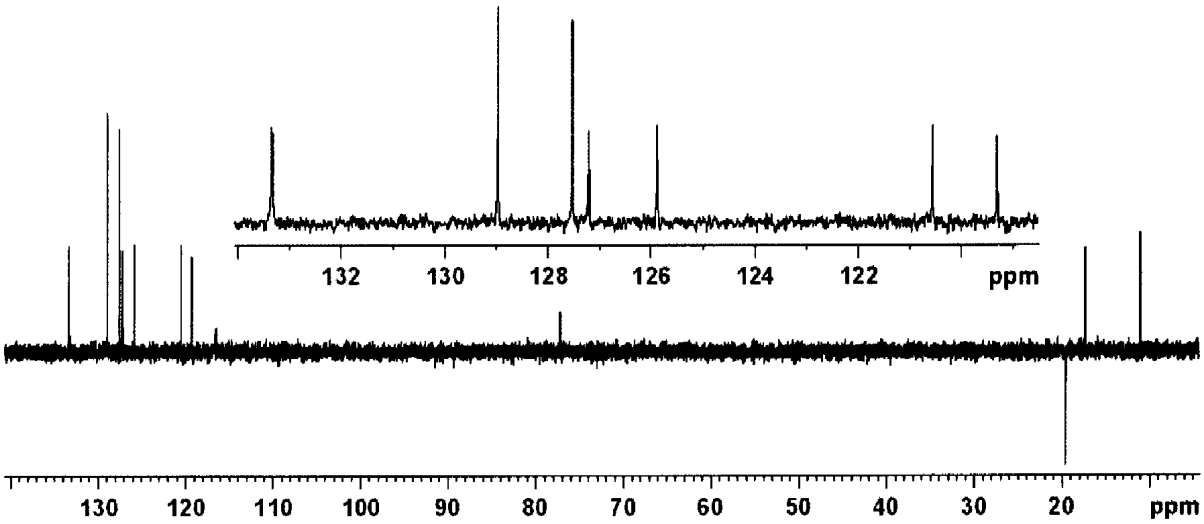

Figure S105. DEPT-135 NMR spectrum of **15d** in $CDCl_3$.

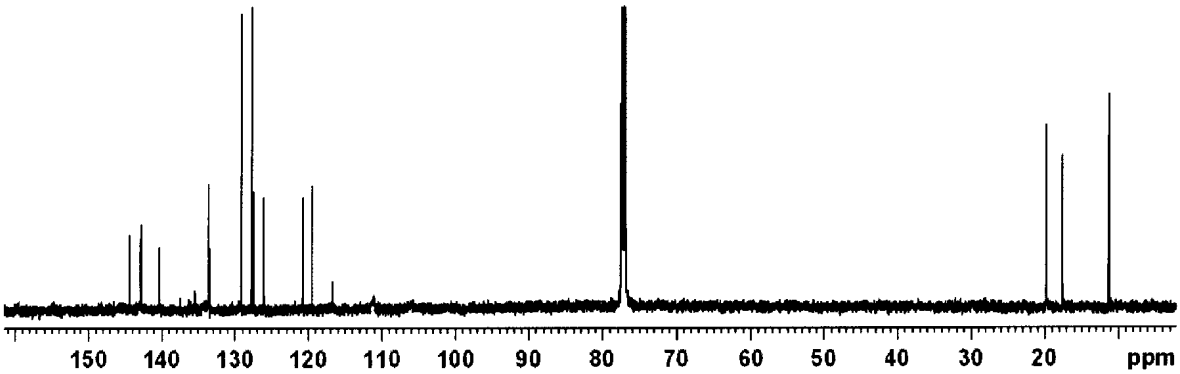

Figure S106. 125 MHz carbon-13 NMR spectrum of phenyl benzoselenacarbaporphyrin **15d** in $CDCl_3$ at 50 ^{o}C.

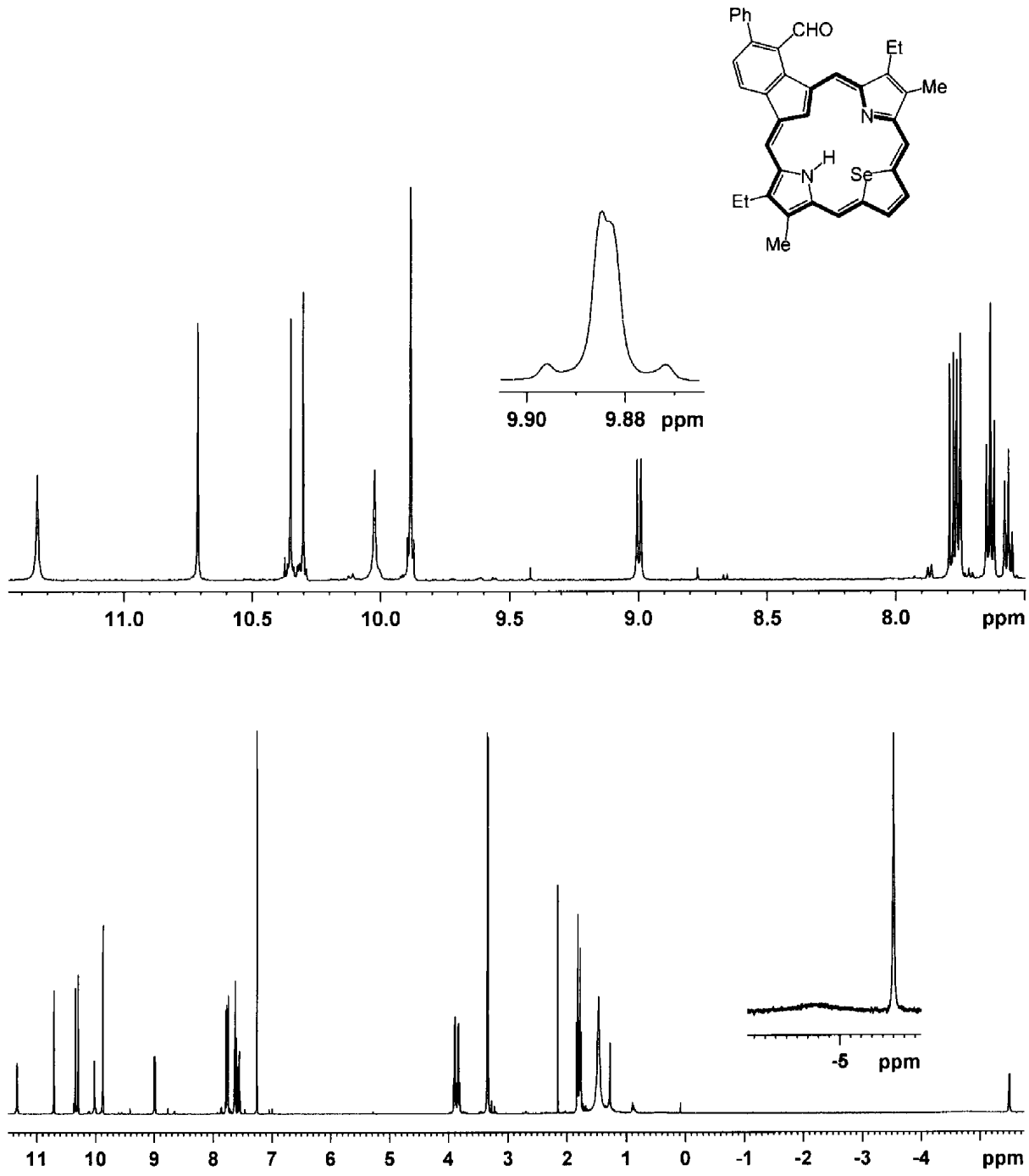

Figure S107. 500 MHz proton NMR spectrum of phenyl benzoselenacarbaporphyrin aldehyde **16d** in $CDCl_3$ at 50 ^{o}C.

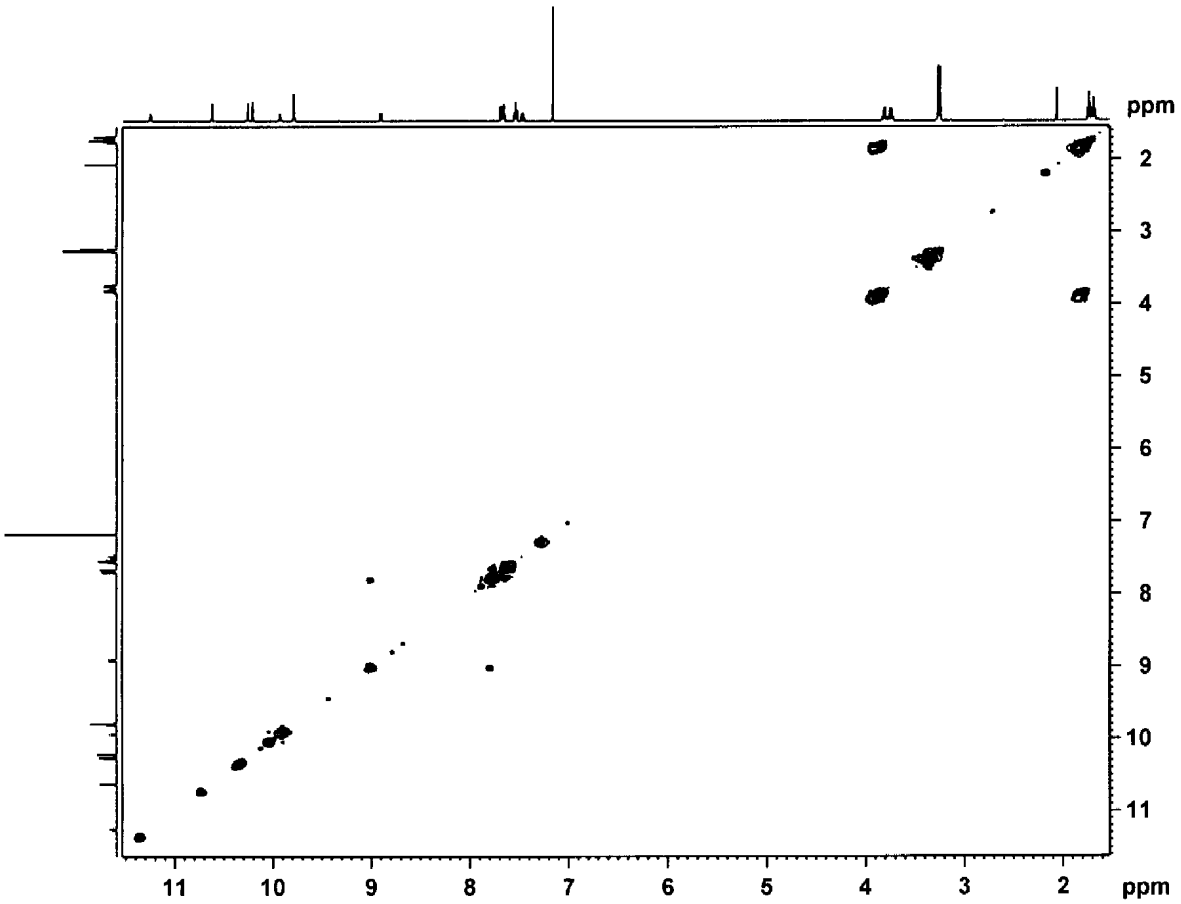

Figure S108. ^{1}H-^{1}H COSY NMR spectrum of phenyl benzoselenacarbaporphyrin aldehyde **16d** in $CDCl_3$.

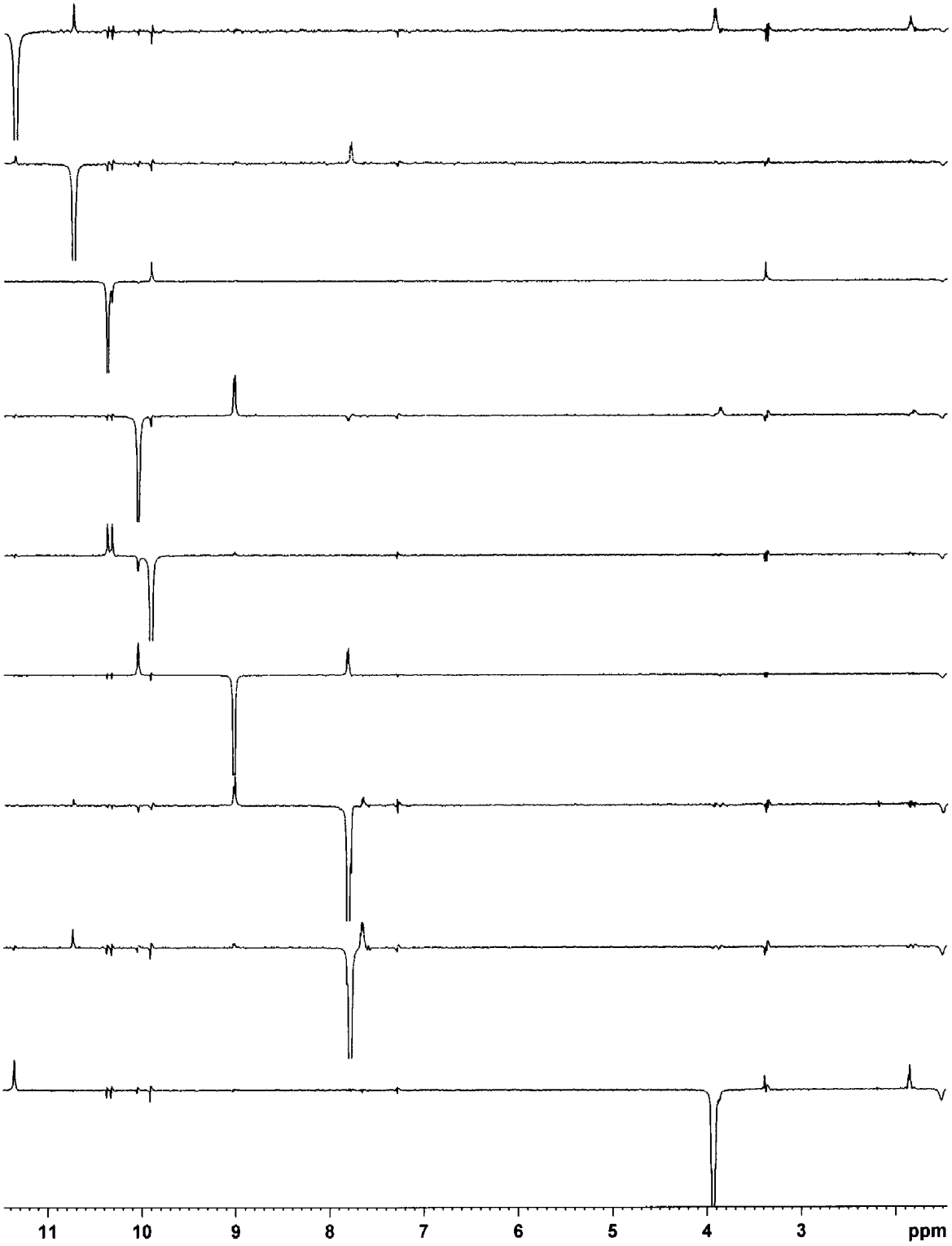

Figure S109. Selected nOe difference proton NMR spectra of **16d** in $CDCl_3$.

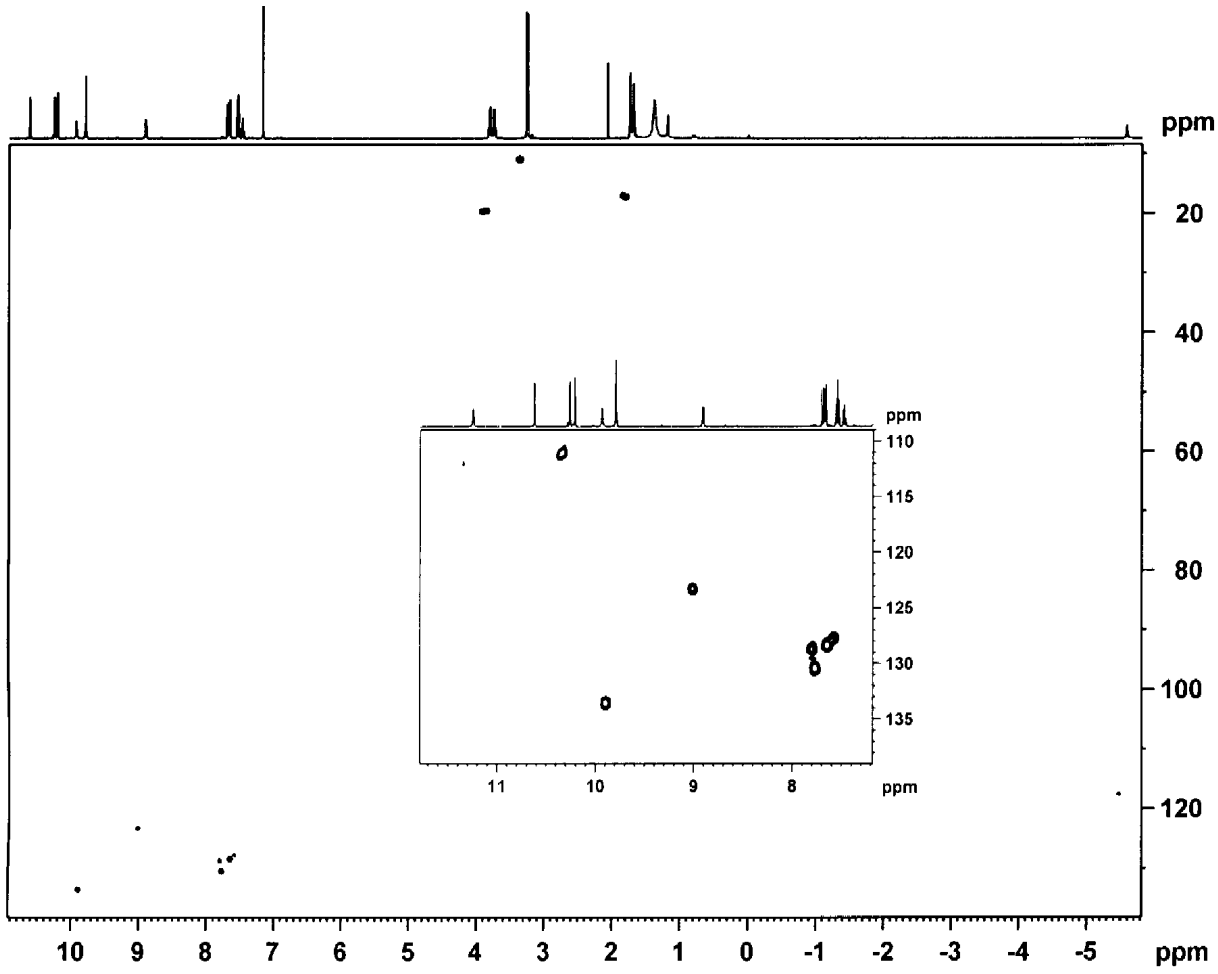

Figure S110. HSQC NMR spectrum of selenacarbaporphyrin aldehyde **16d** in $CDCl_3$.

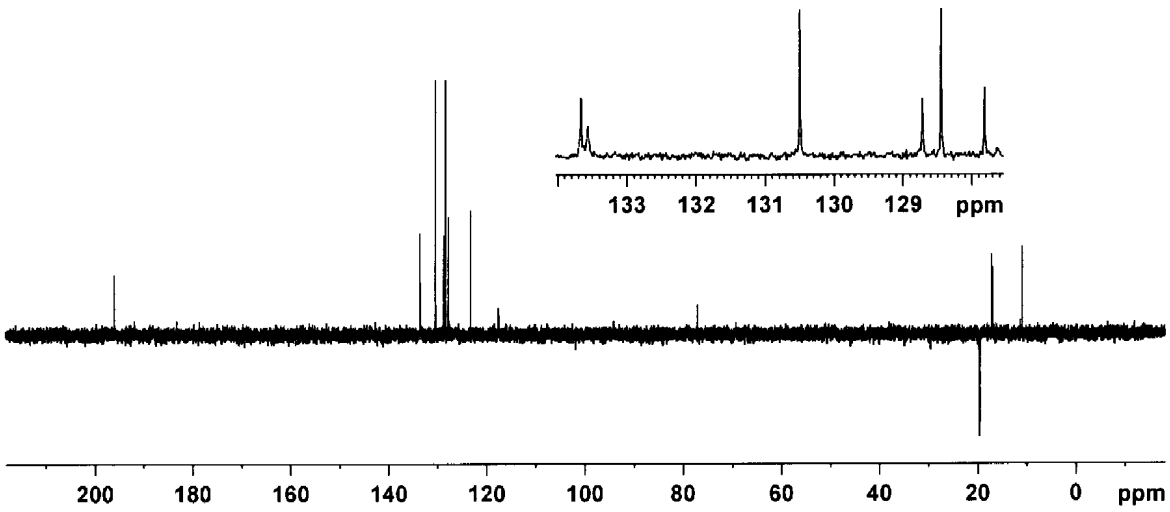

Figure S111. DEPT-135 NMR spectrum of **16d** in $CDCl_3$.

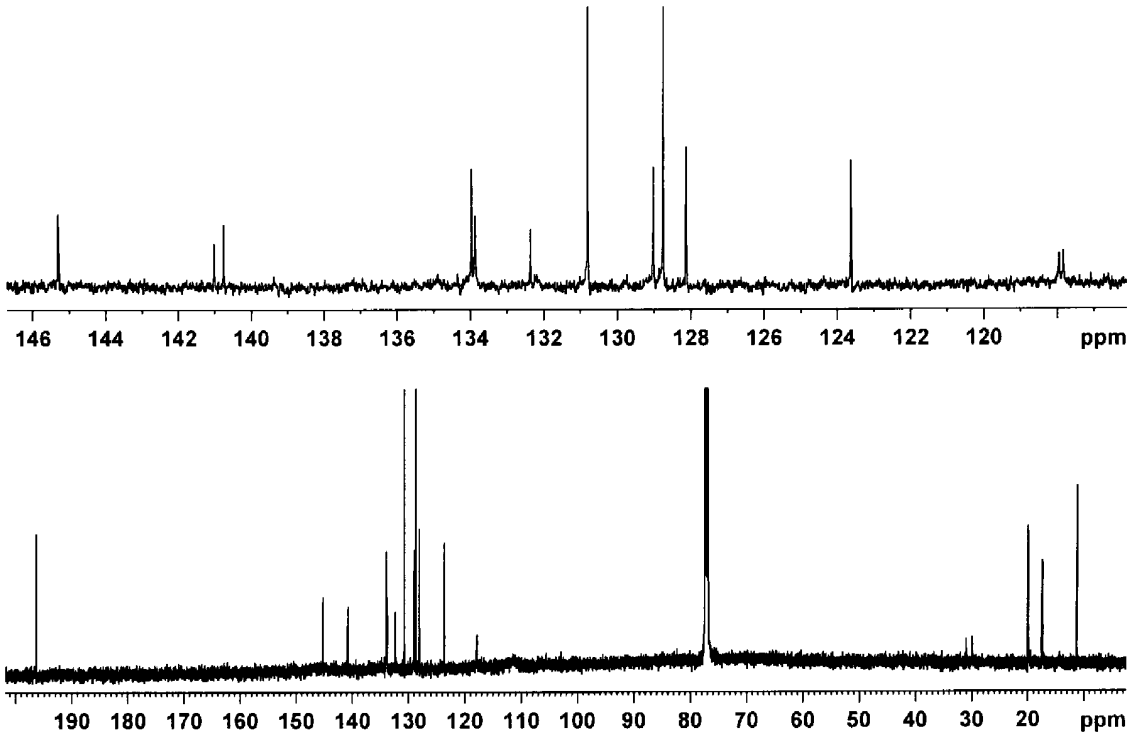

Figure S112. 125 MHz carbon-13 NMR spectrum of selenacarbaporphyrin aldehyde **16d** in $CDCl_3$ at 50 ^{o}C.

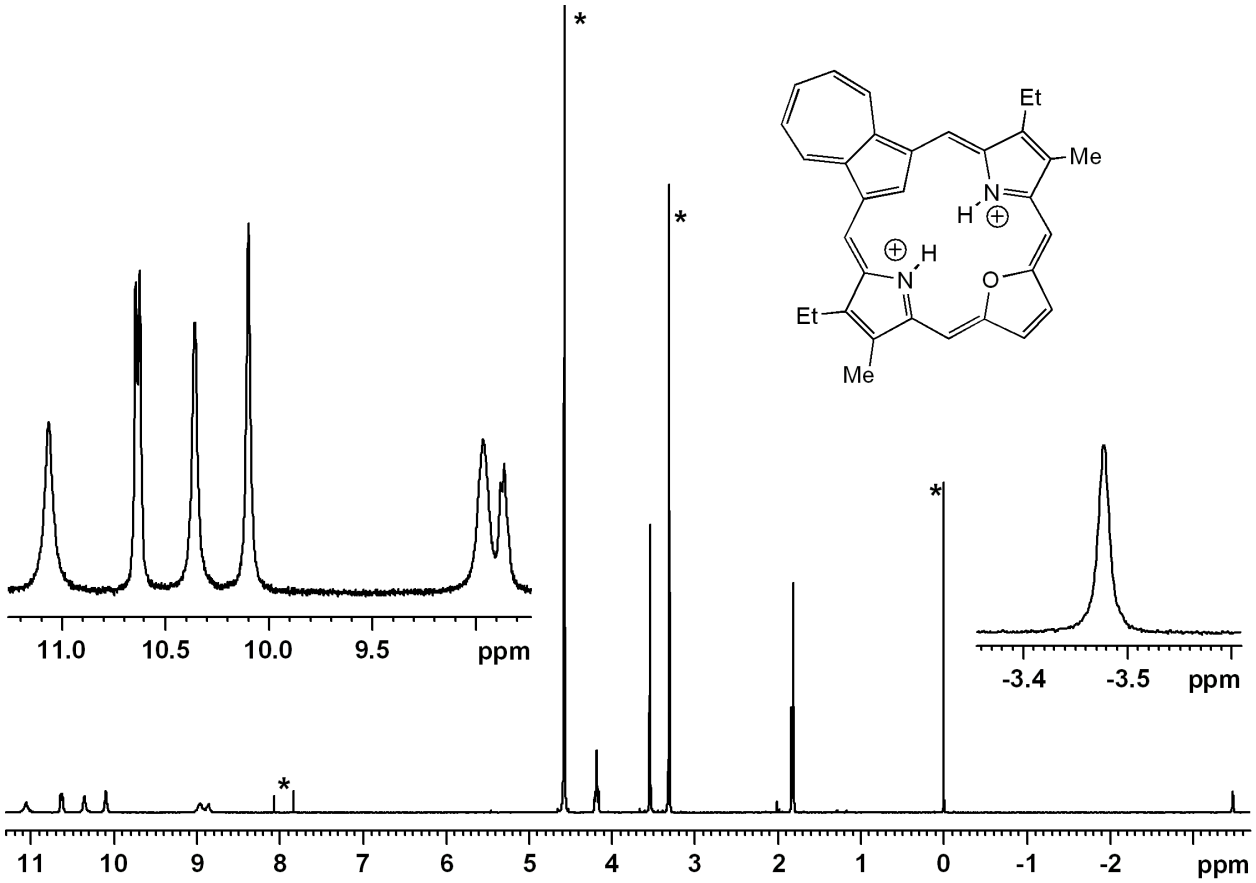

Figure S113. 500 MHz proton NMR spectrum of oxa-azuliporphyrin **12a**.2HCl in methanol-d_4 at 50 ^{o}C. * = solvent impurities.

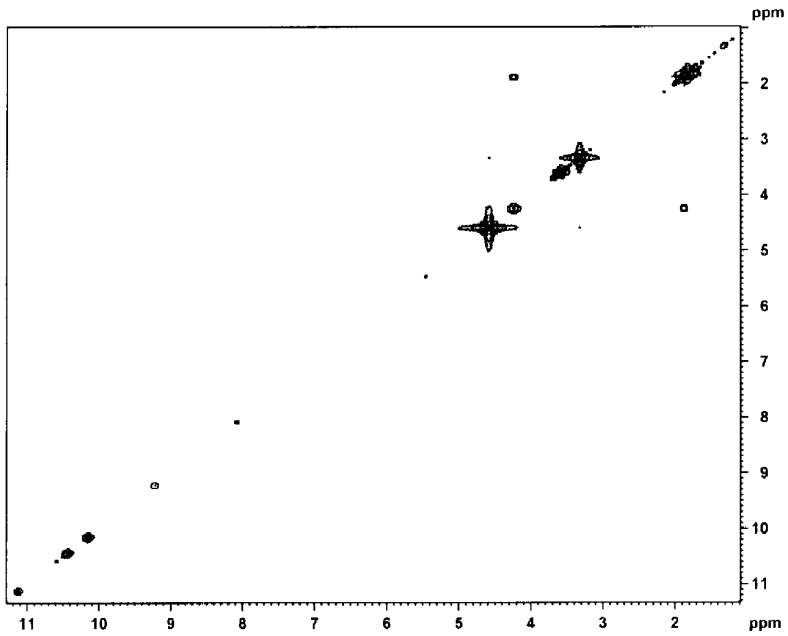

Figure S114. ^{1}H-^{1}H COSY NMR spectrum of **12a**.2HCl in methanol-d_4.

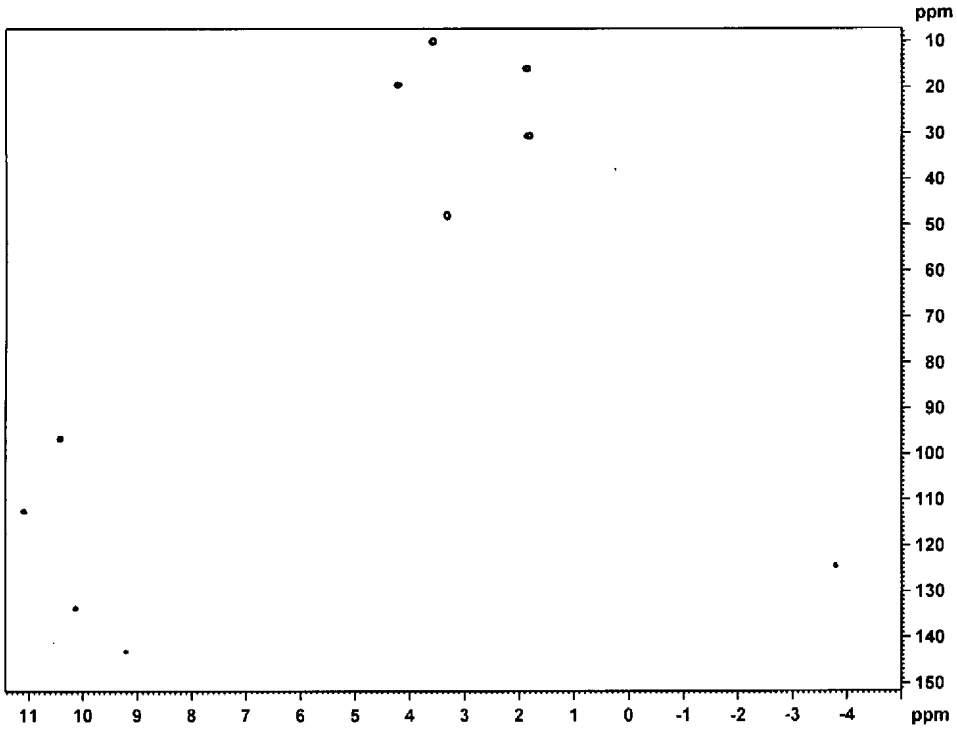

Figure S115. HSQC NMR spectrum of **12a**.2HCl in methanol-d_4.

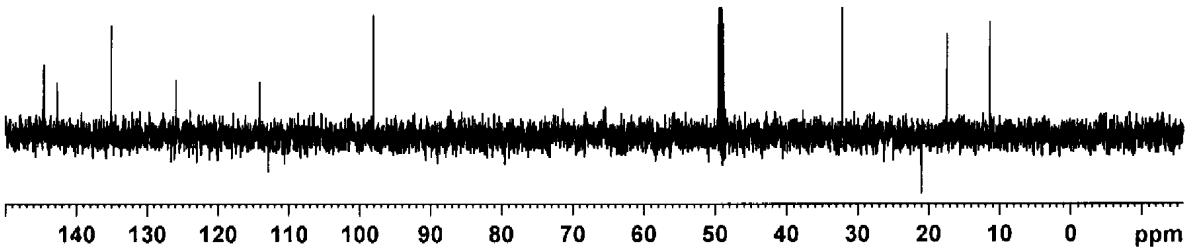

Figure S116. DEPT-135 NMR spectrum of **12a**.2HCl in methanol-d_4.

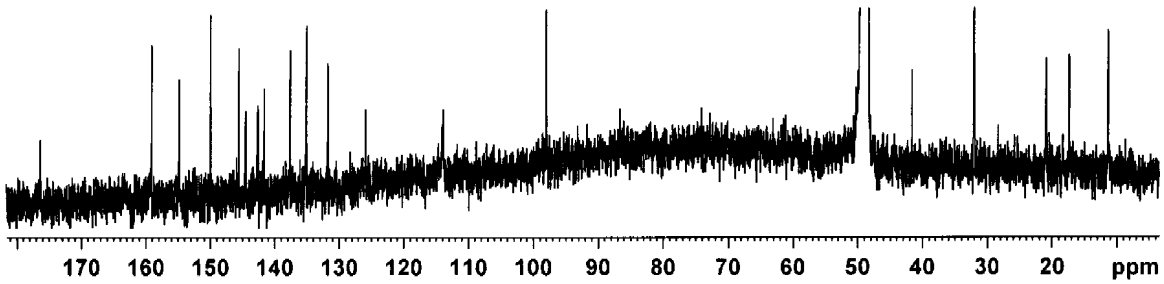

Figure S117. 125 MHz carbon-13 NMR spectrum of **12a**.2HCl in methanol-d_4 at 50 ^{o}C. The poor quality of the spectrum is due to the very poor solubility of this sample.

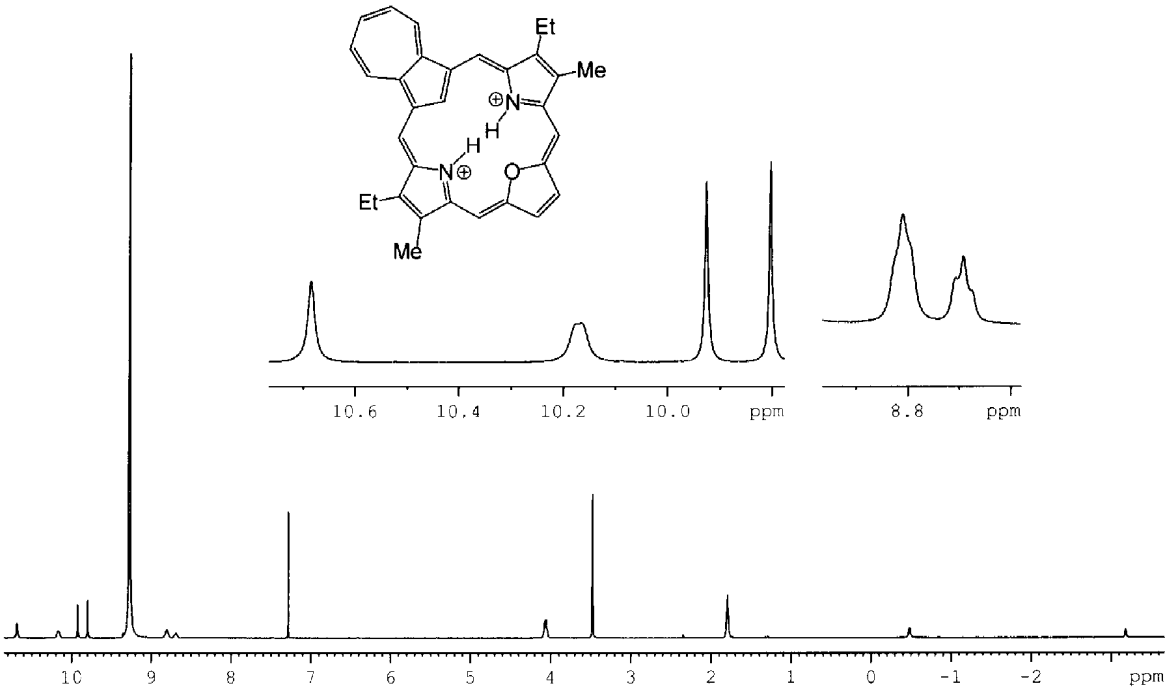

Figure S118. 500 MHz proton NMR spectrum of **12a**.2HCl in TFA-$CDCl_3$.

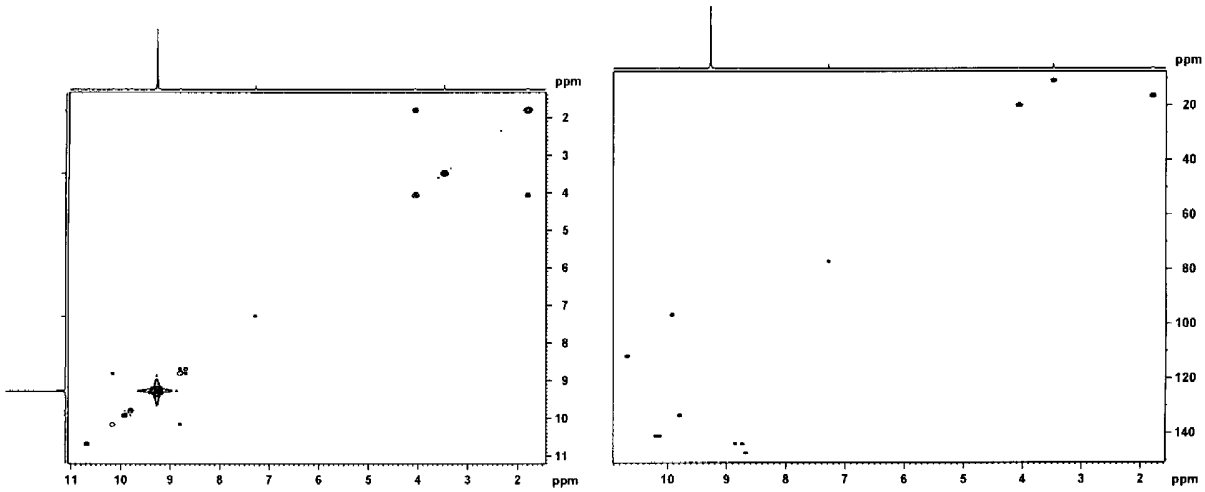

Figure S119. ^{1}H-^{1}H COSY (left) and HSQC (right) NMR spectra of **12a**.2HCl in TFA-$CDCl_3$.

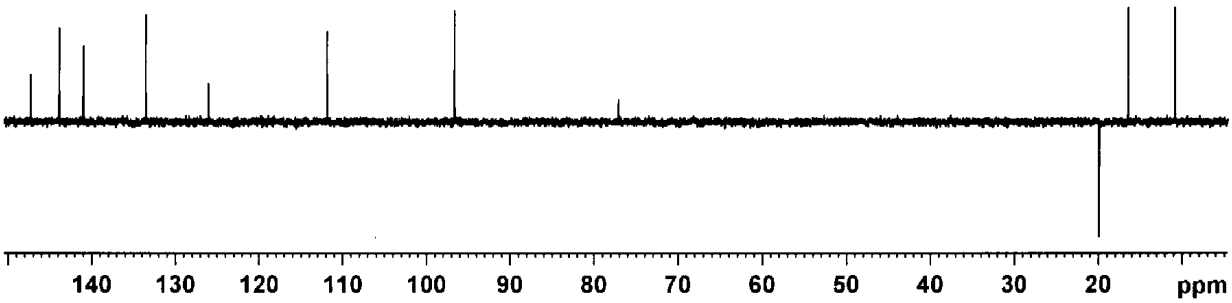

Figure S120. DEPT-135 NMR spectrum of **12a**.2HCl in TFA-$CDCl_3$.

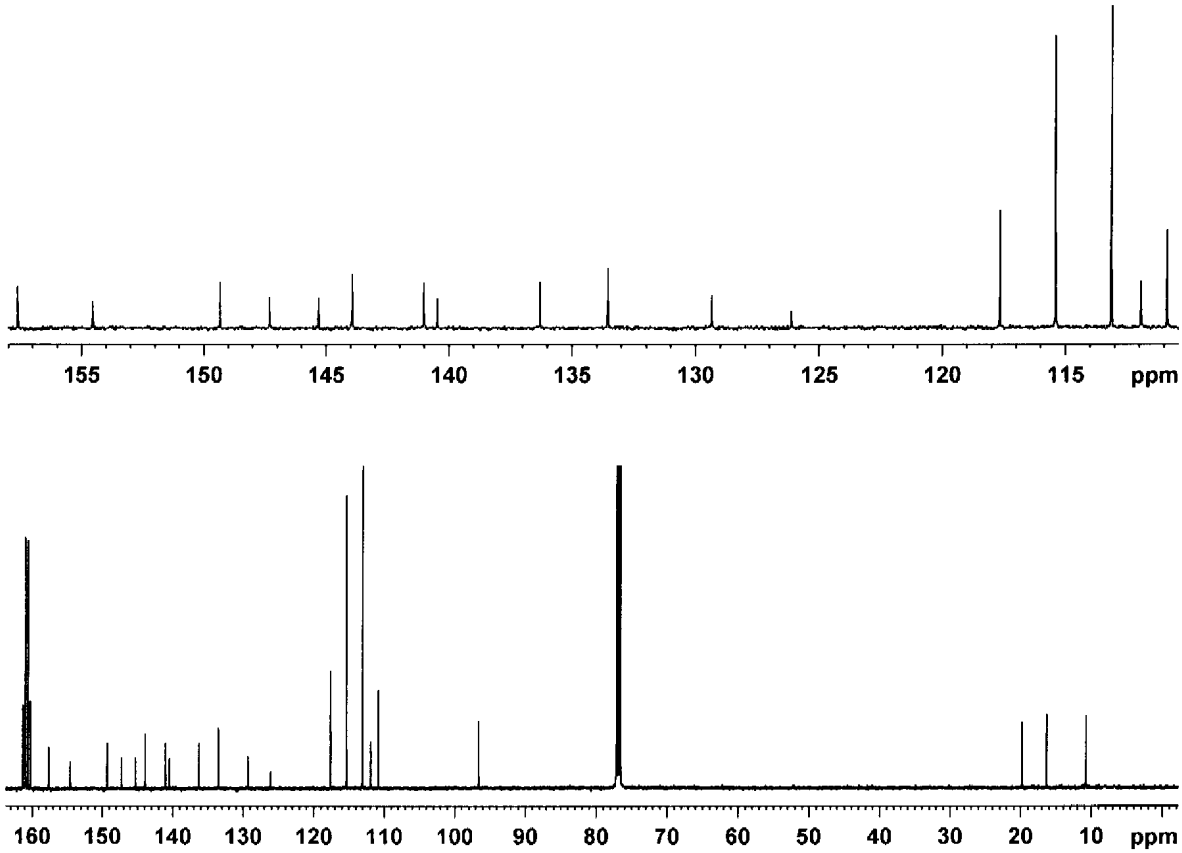

Figure S121. 125 MHz proton NMR spectrum of **12a**.2HCl in TFA-$CDCl_3$.

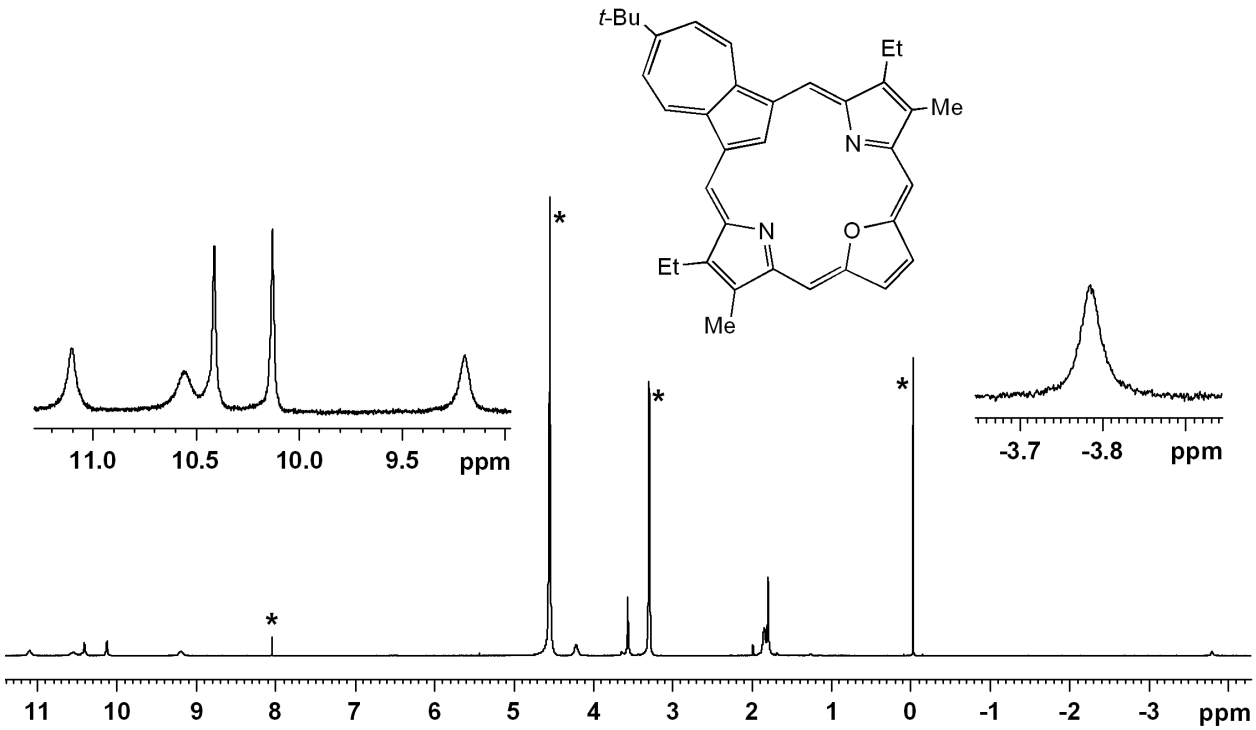

Figure S122. 500 MHz proton NMR spectrum of *tert*-butyl oxa-azuliporphyrin **12b**.2HCl in methanol-d_4. * = solvent impurities.

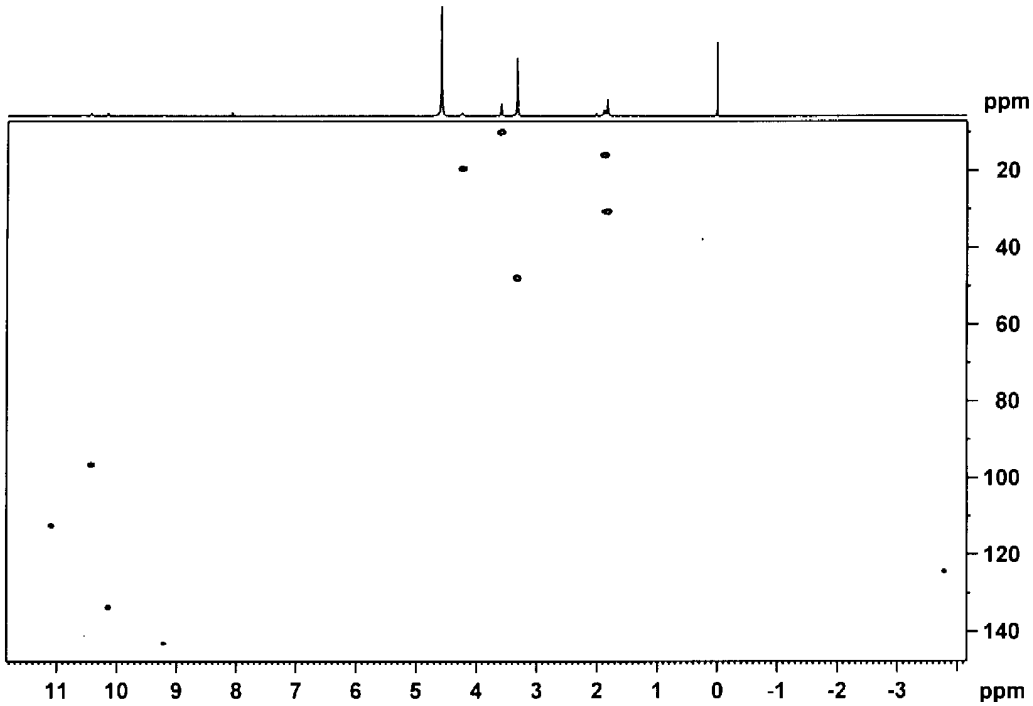

Figure S123. HSQC NMR spectrum of **12b**.2HCl in methanol-d_4.

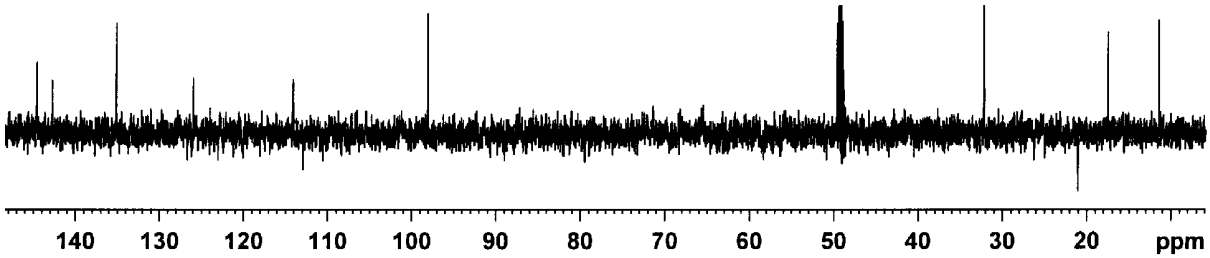

Figure S124. DEPT-135 NMR spectrum of **12b**.2HCl in methanol-d_4.

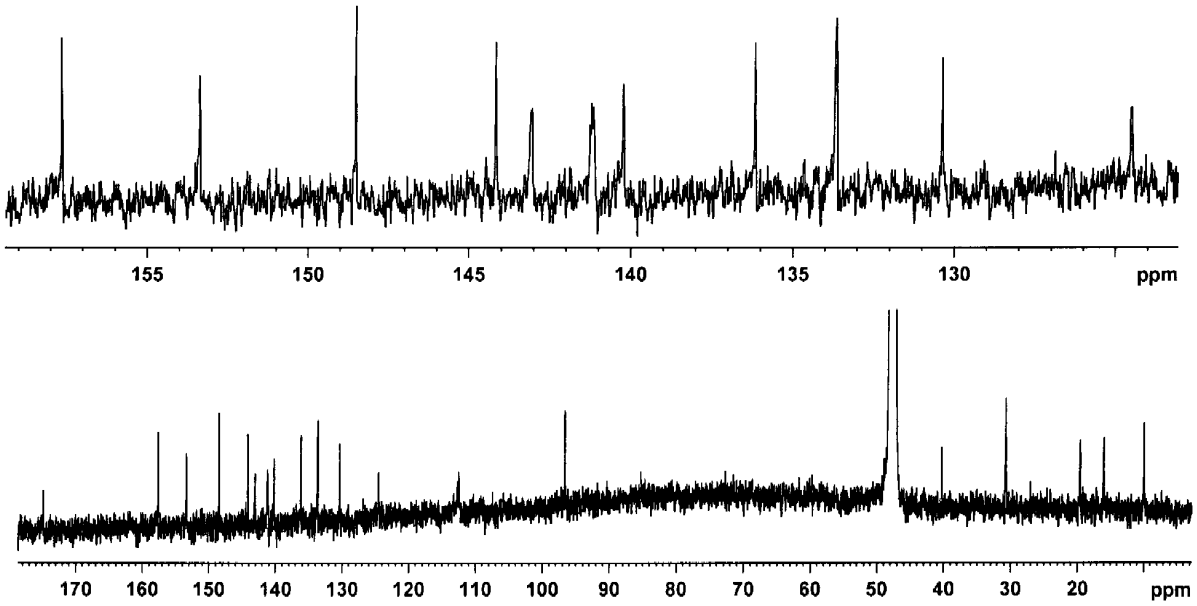

Figure S125. 125 MHz carbon-13 NMR spectrum of **12b**.2HCl in methanol-d_4. The poor quality of the spectrum is due to the very poor solubility of this sample.

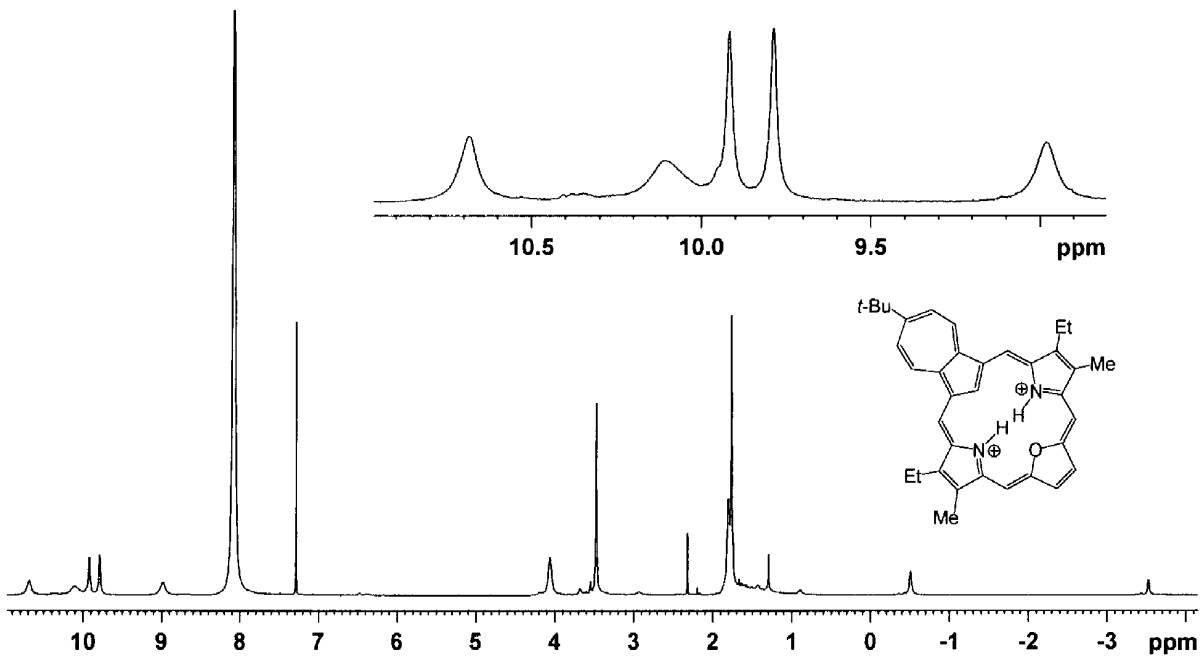

Figure S126. 500 MHz proton NMR spectrum of *tert*-butyl oxa-azuliporphyrin **12b**.2HCl in TFA-$CDCl_3$.

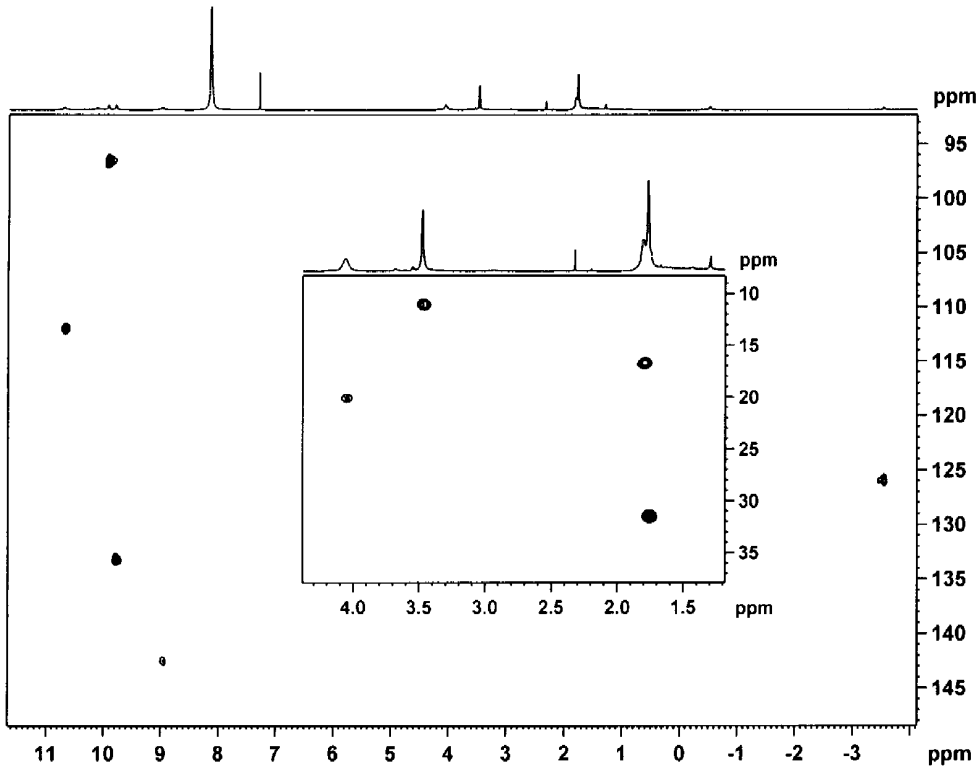

Figure S127. HSQC NMR spectrum of **12b**.2HCl in TFA-$CDCl_3$.

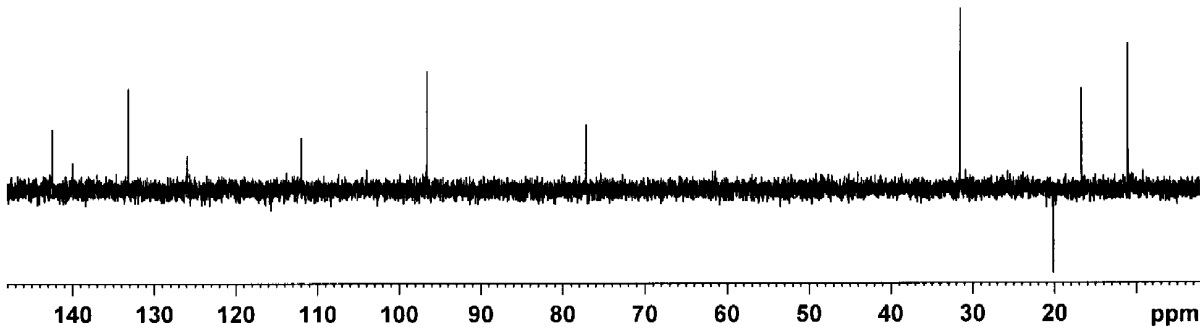

Figure S128. DEPT-135 NMR spectrum of **12b**.2HCl in TFA-$CDCl_3$.

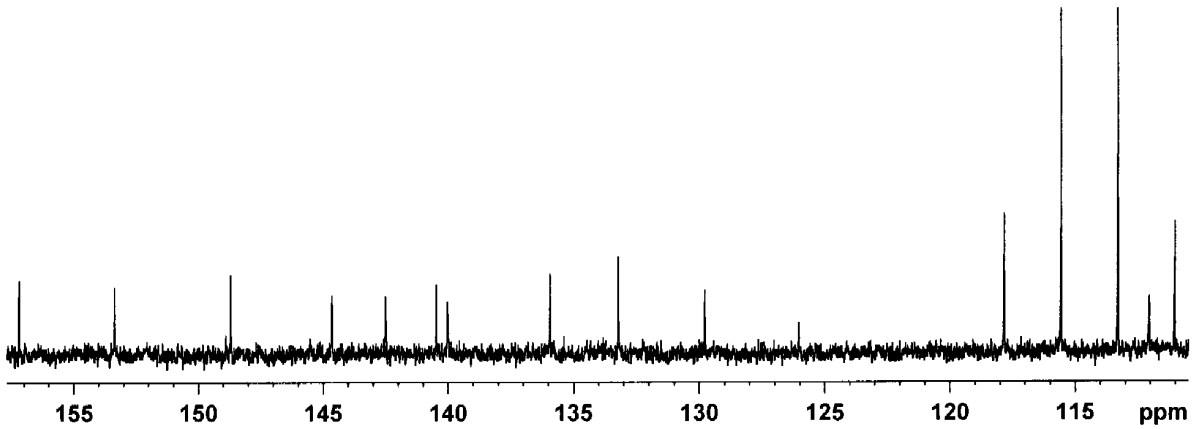

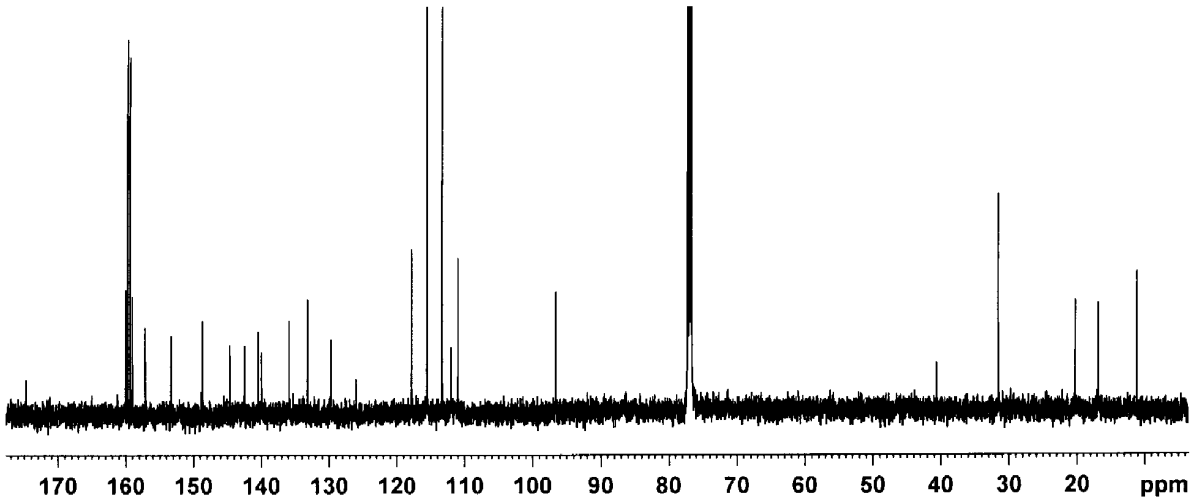

Figure S129. 125 MHz carbon-13 NMR spectrum of **12b**.2HCl in TFA-$CDCl_3$.

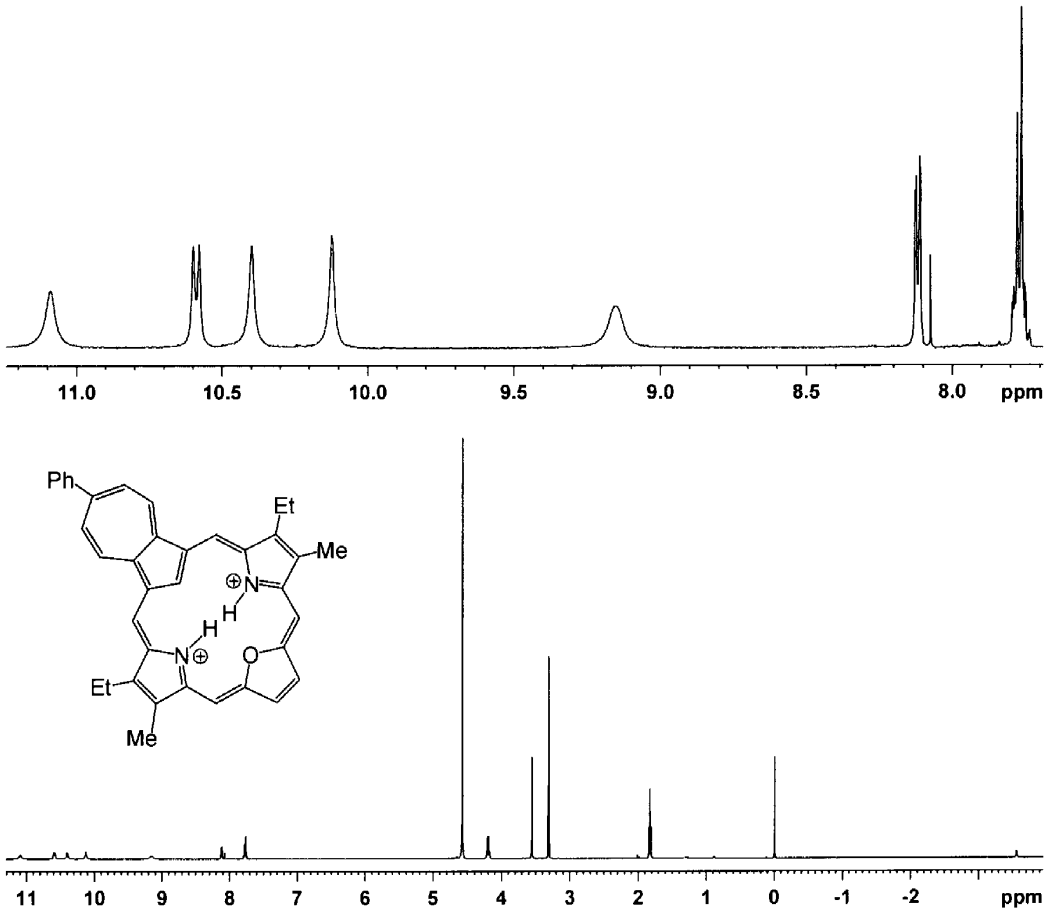

Figure S130. 500 MHz proton NMR spectrum of phenyl oxa-azuliporphyrin **12c**.2HCl in methanol-d_4. * = solvent impurities.

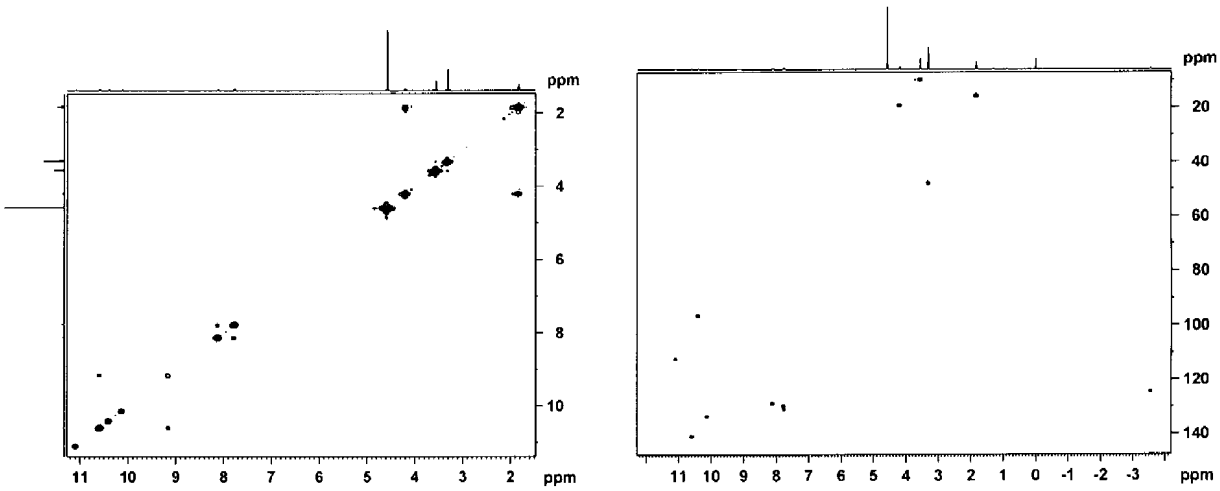

Figure S131. ^{1}H-^{1}H COSY (left) and HSQC (right) NMR spectra of **12c**.2HCl in methanol-d_4.

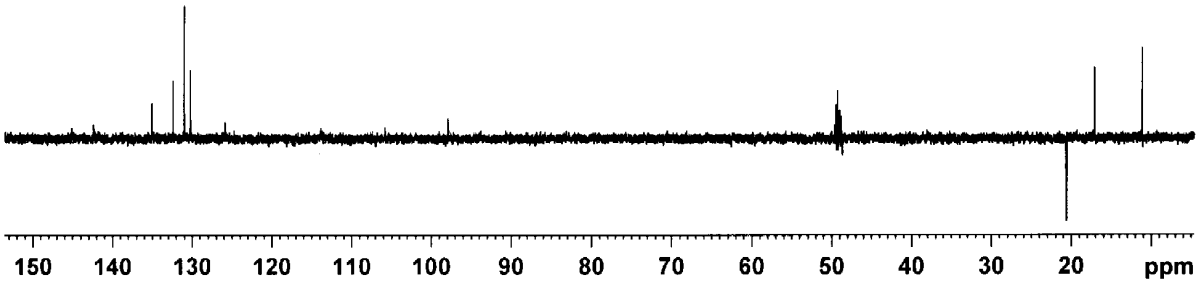

Figure S132. DEPT-135 NMR spectrum of **12c**.2HCl in methanol-d_4.

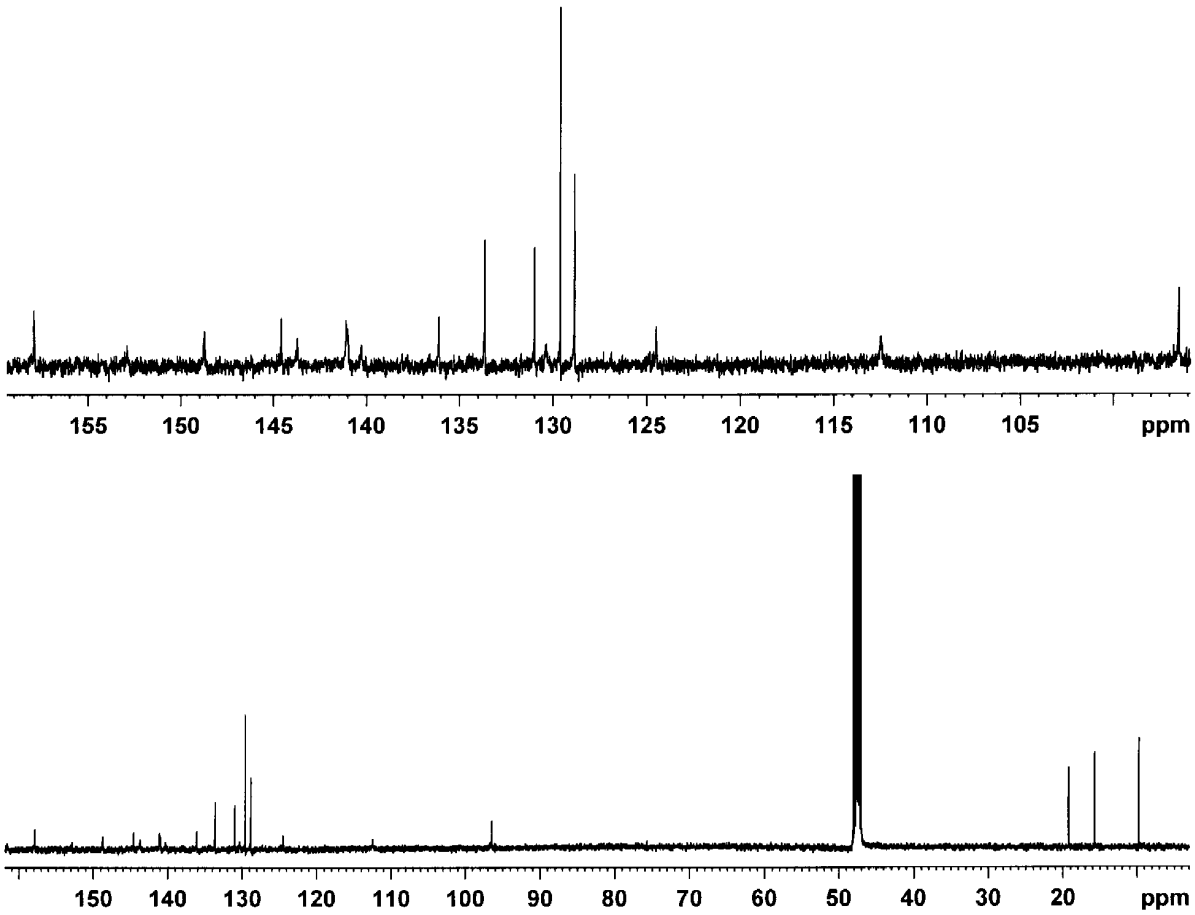

Figure S133. 125 MHz carbon-13 NMR spectrum of **12c**.2HCl in methanol-d_4. The poor quality of the spectrum is due to the very poor solubility of this sample.

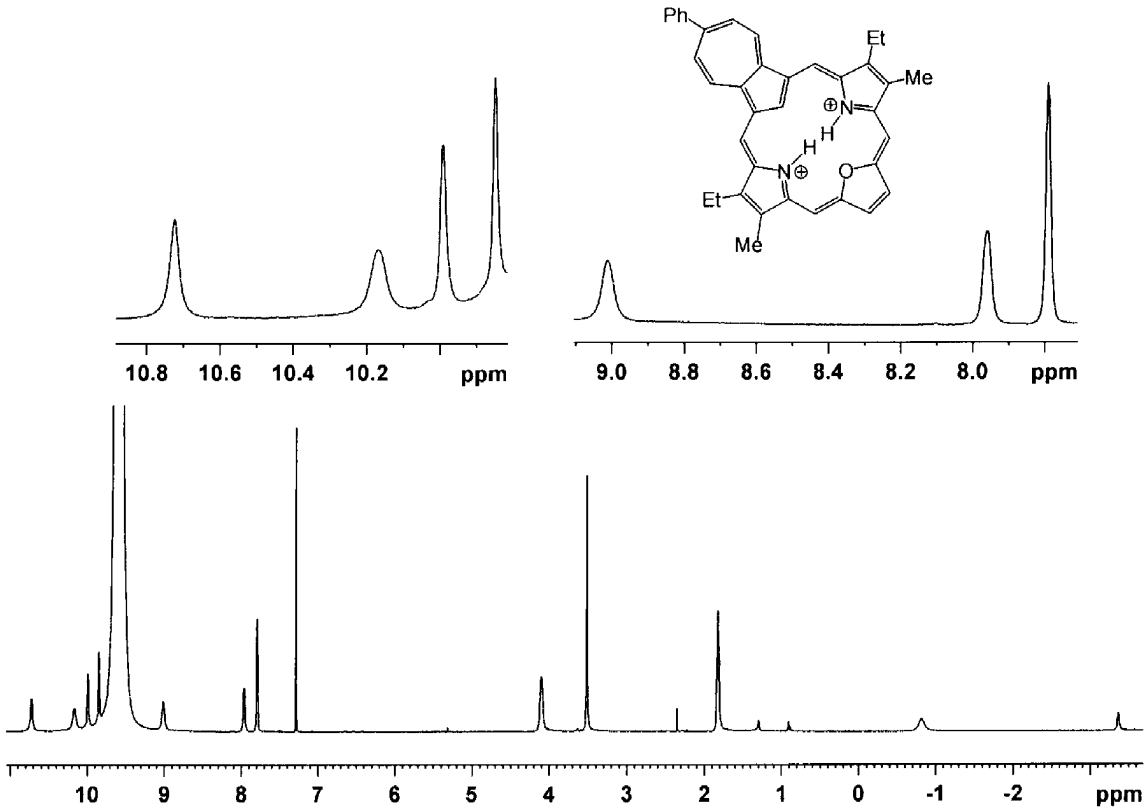

Figure S134. 500 MHz proton NMR spectrum of phenyl oxa-azuliporphyrin **12c**.2HCl in TFA-$CDCl_3$.

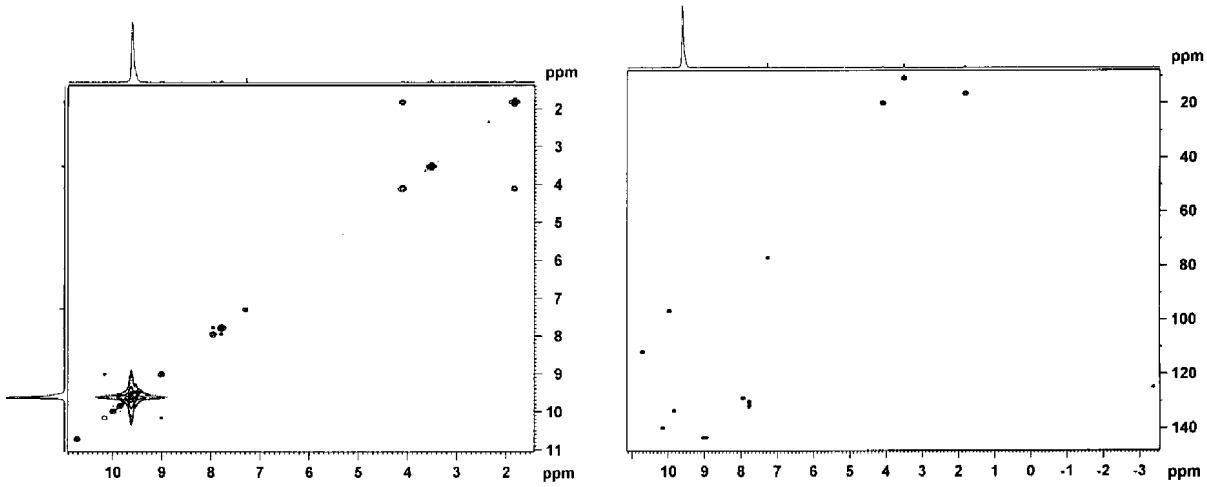

Figure S135. ^{1}H-^{1}H COSY (left) and HSQC (right) NMR spectra of **12c**.2HCl in TFA-$CDCl_3$.

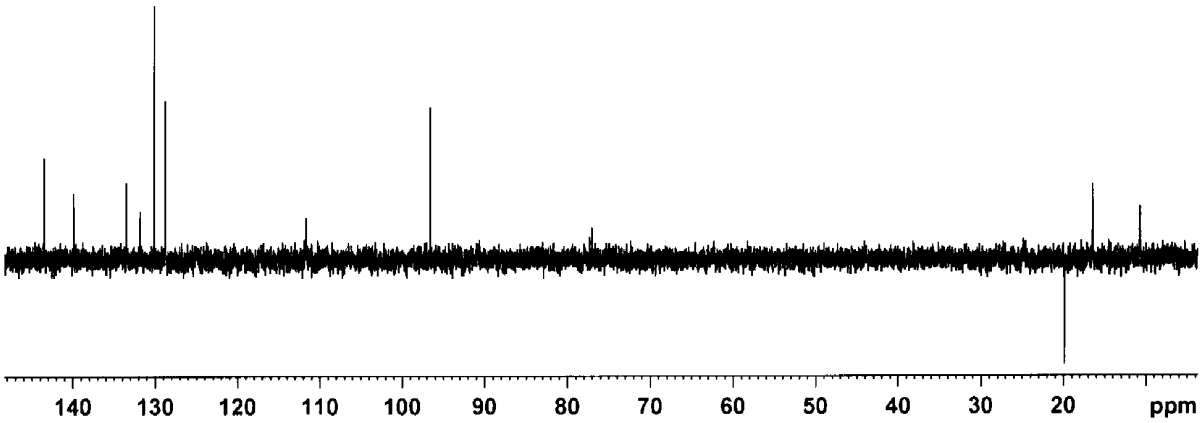

Figure S136. DEPT-135 NMR spectrum of **12c**.2HCl in TFA-$CDCl_3$.

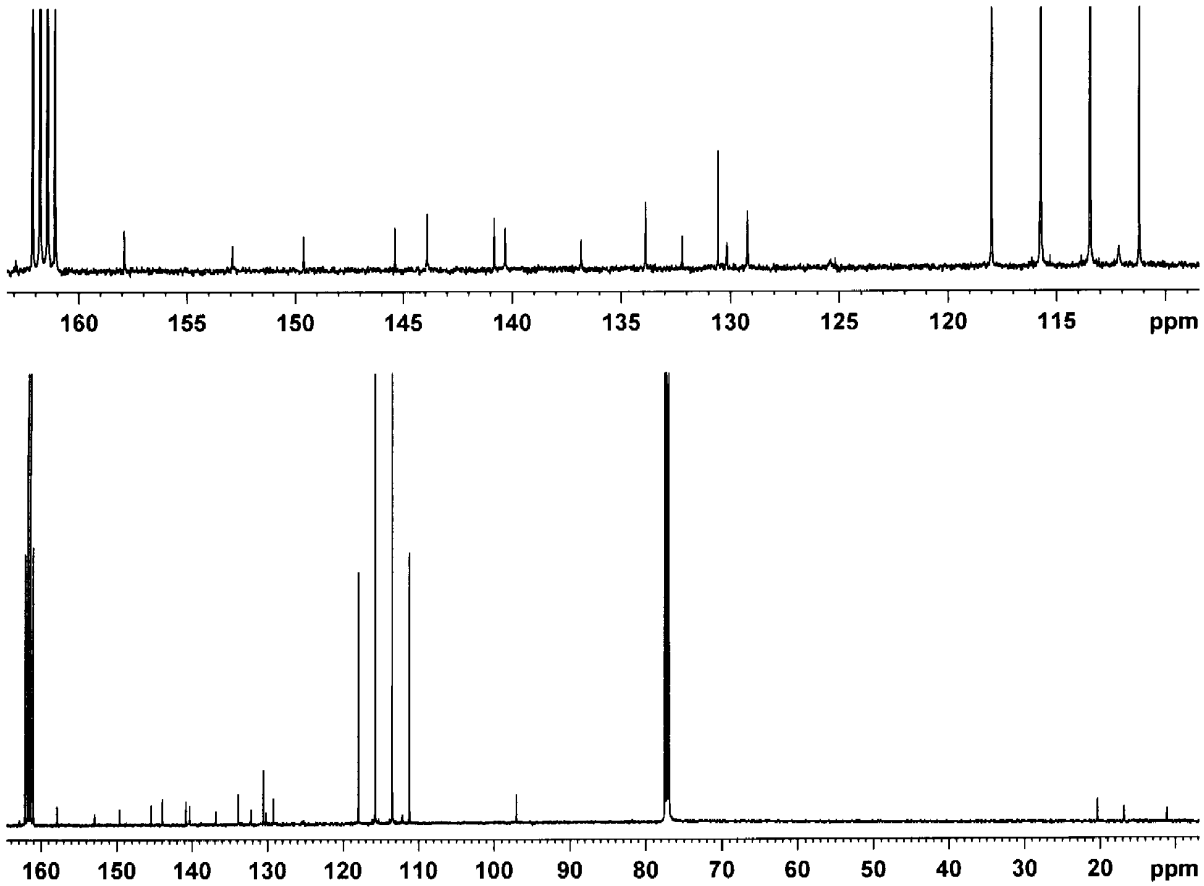

Figure S137. 125 MHz carbon-13 NMR spectrum of **12c**.2HCl in TFA-$CDCl_3$.

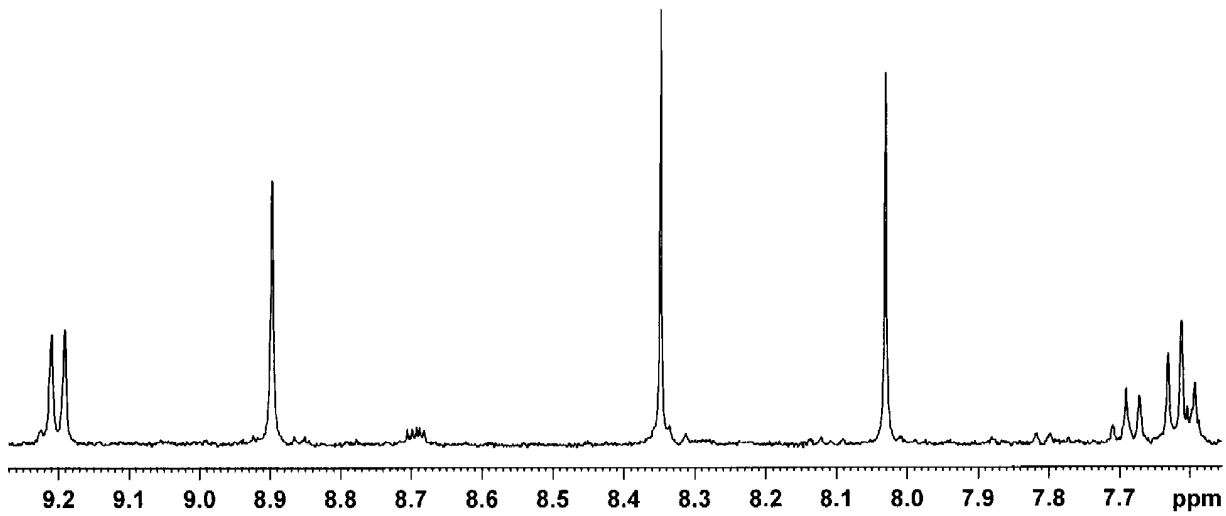

Figure S138. Partial 500 MHz proton NMR spectrum of **12a**.2HCl in DBU-$CDCl_3$. The free base oxa-azuliporphyrin is very unstable and rapidly decomposes.

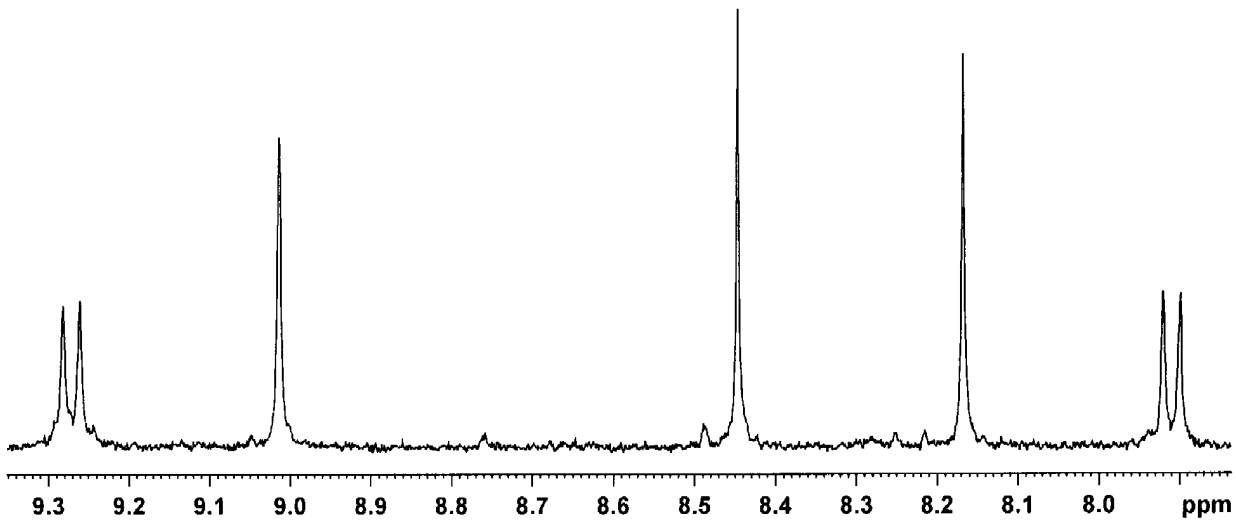

Figure S139. Partial 500 MHz proton NMR spectrum of **12b**.2HCl in DBU-$CDCl_3$. The free base oxa-azuliporphyrin is very unstable and rapidly decomposes.

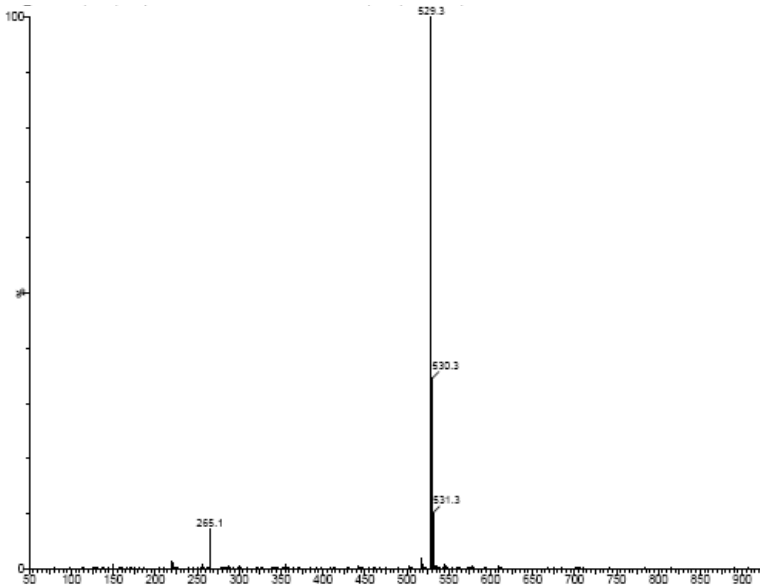

Figure S140. ESI MS of *tert*-butyl thia-azuliporphyrin **8b**.

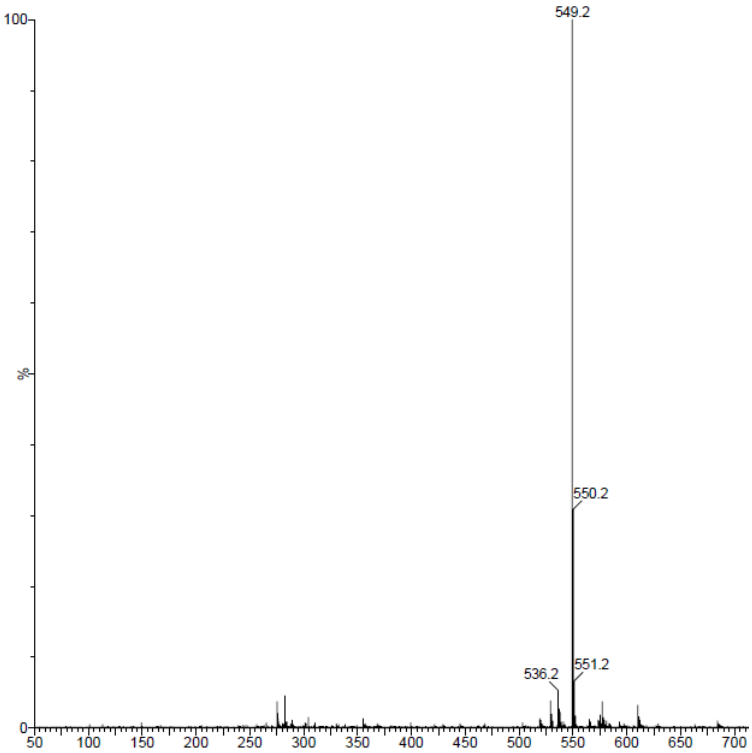

Figure S141. ESI MS of phenyl thia-azuliporphyrin **8c**.

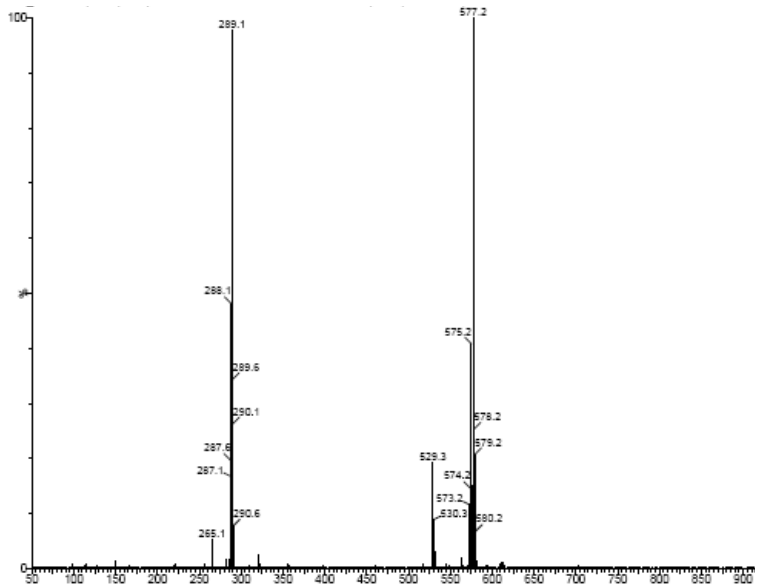

Figure S142. ESI MS of *tert*-butyl selena-azuliporphyrin **9b**.

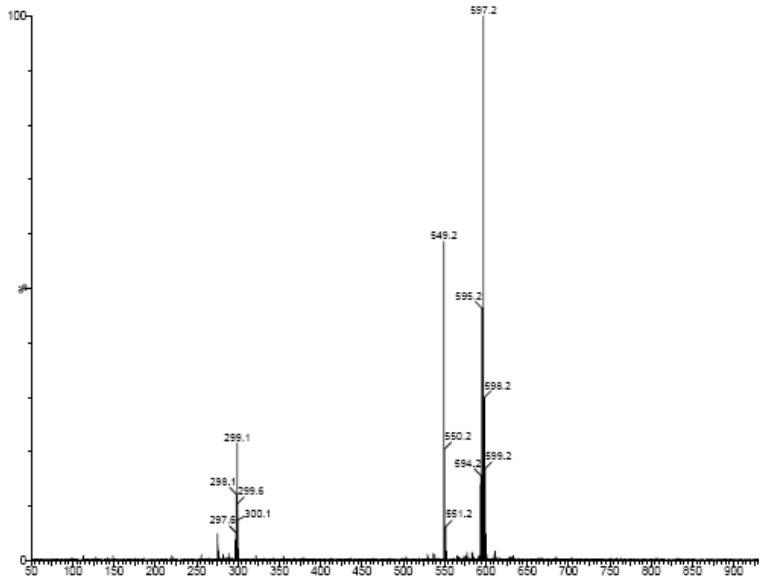

Figure S143. ESI MS of phenyl selena-azuliporphyrin **9c**.

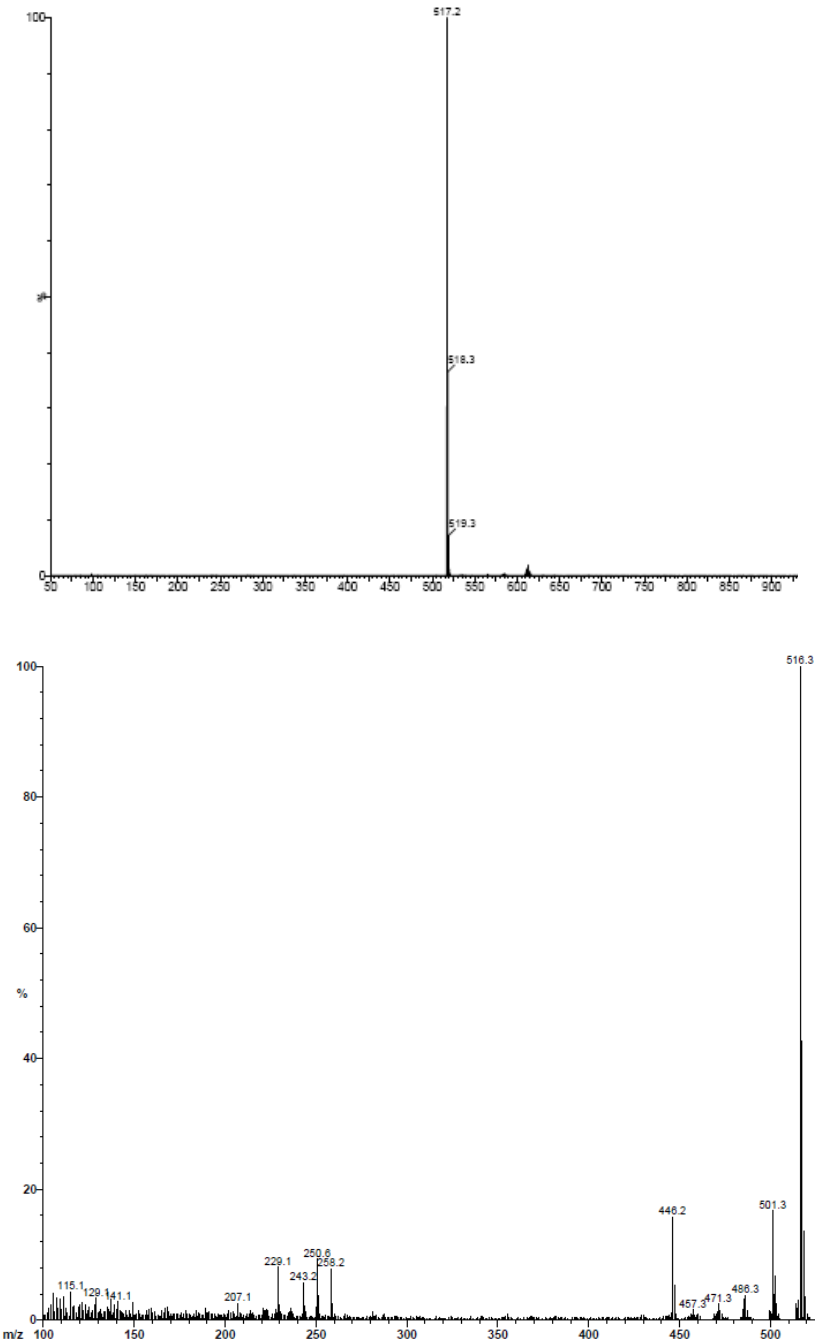

Figure S144. ESI (top) and electron impact (bottom) mass spectra of *tert*-butyl benzothiacarbaporphyrin **15a**.

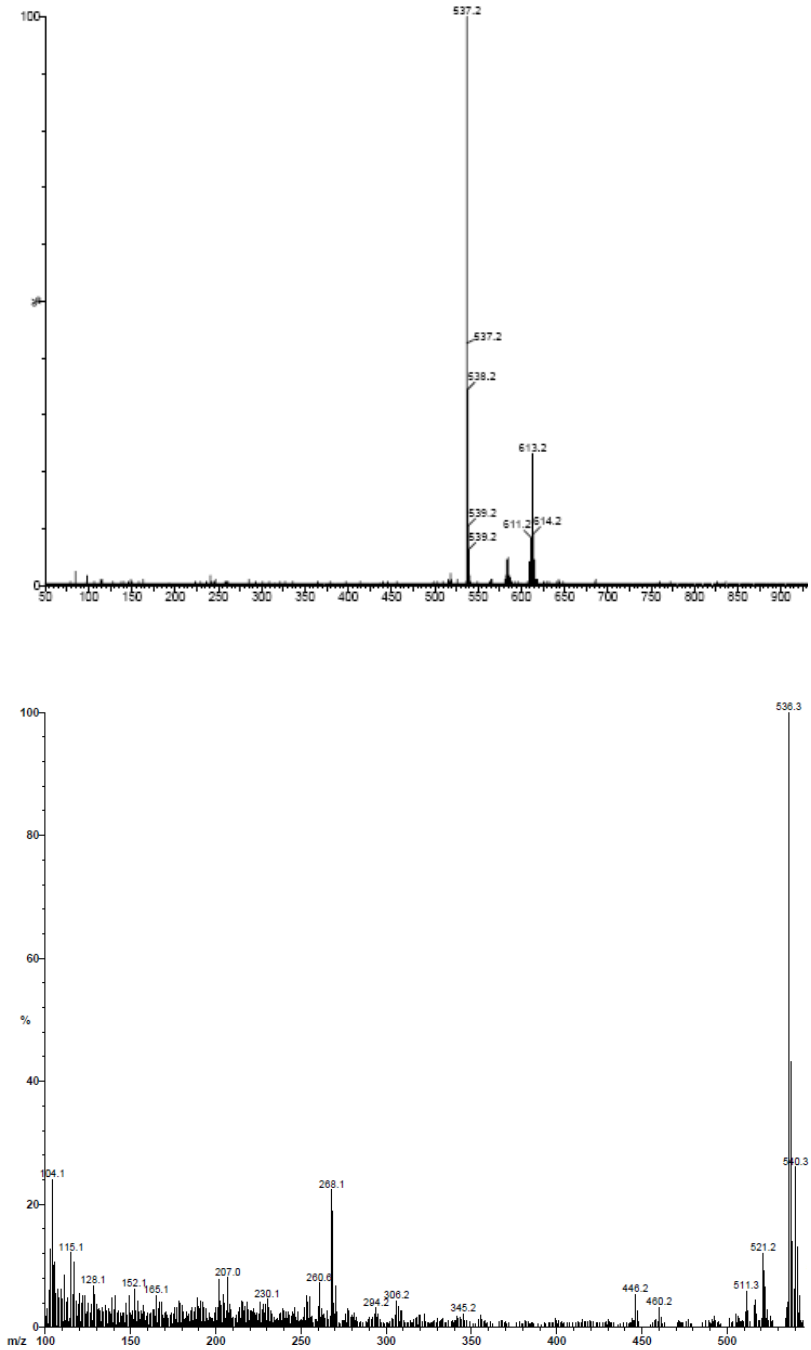

Figure S145. ESI (top) and electron impact (bottom) mass spectra of phenyl benzothiacarbaporphyrin **15b**.

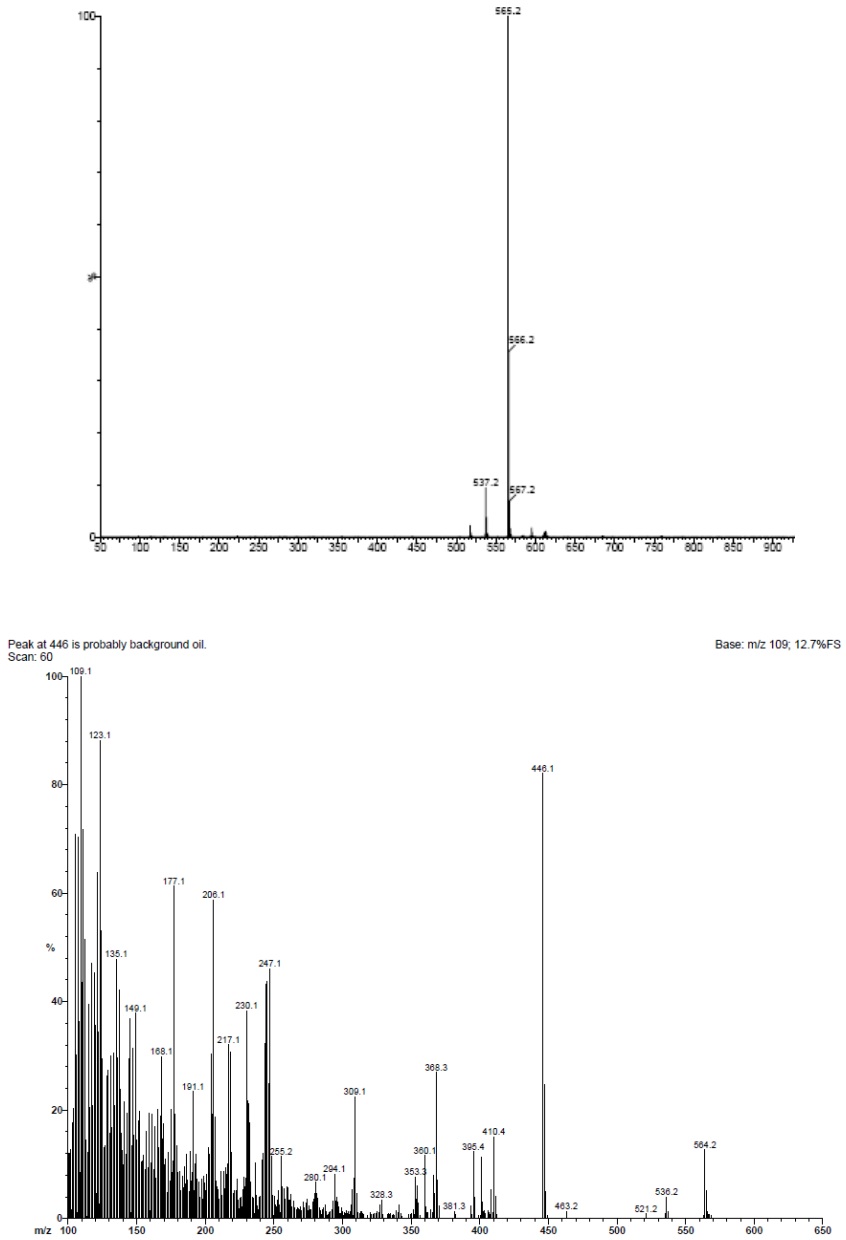

Figure S146. ESI (top) and electron impact (bottom) mass spectra of phenyl benzothiacarbaporphyrin aldehyde **16b**.

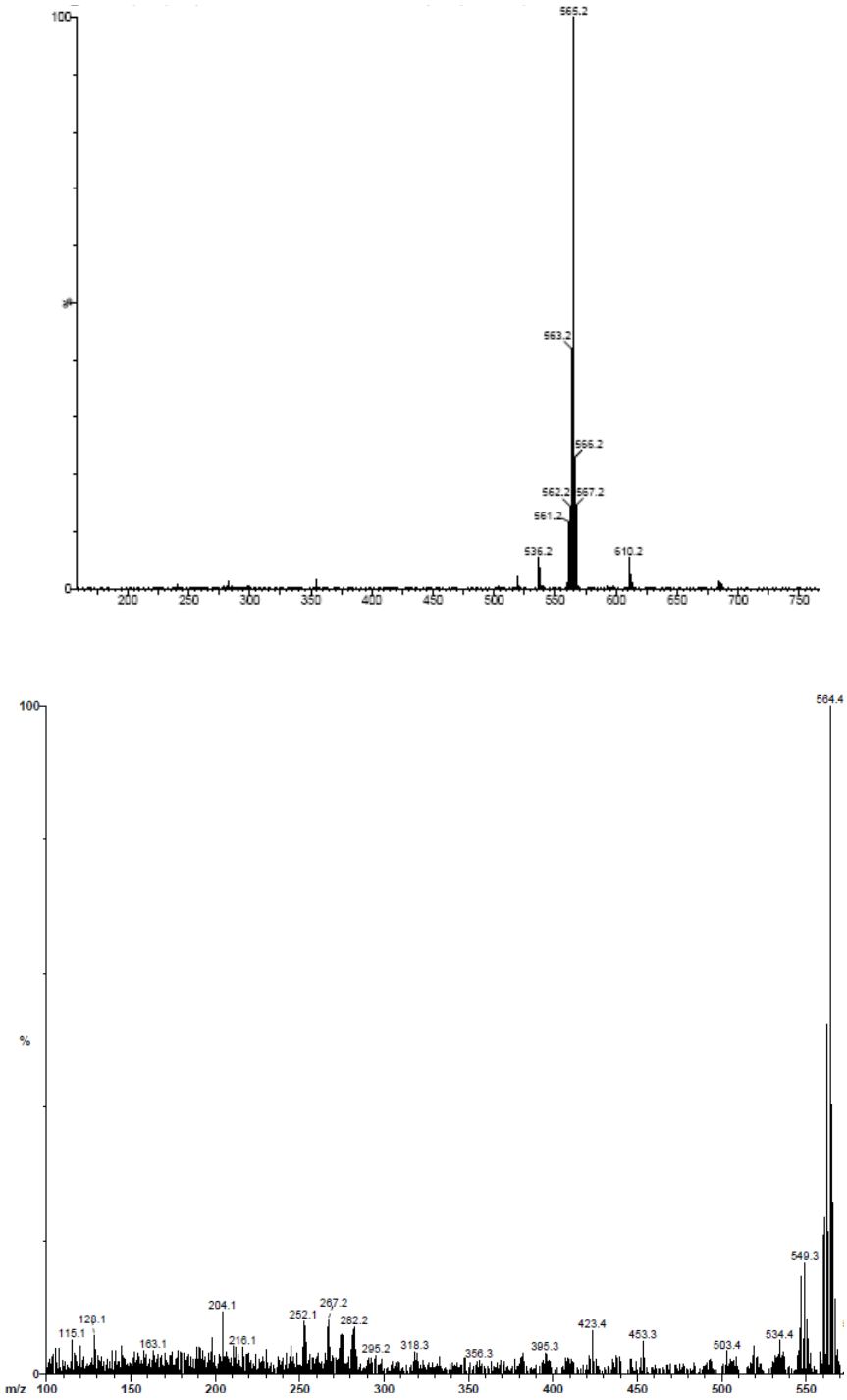

Figure S147. ESI (top) and electron impact (bottom) mass spectra of *tert*-butyl benzoselenacarbaporphyrin **15c**.

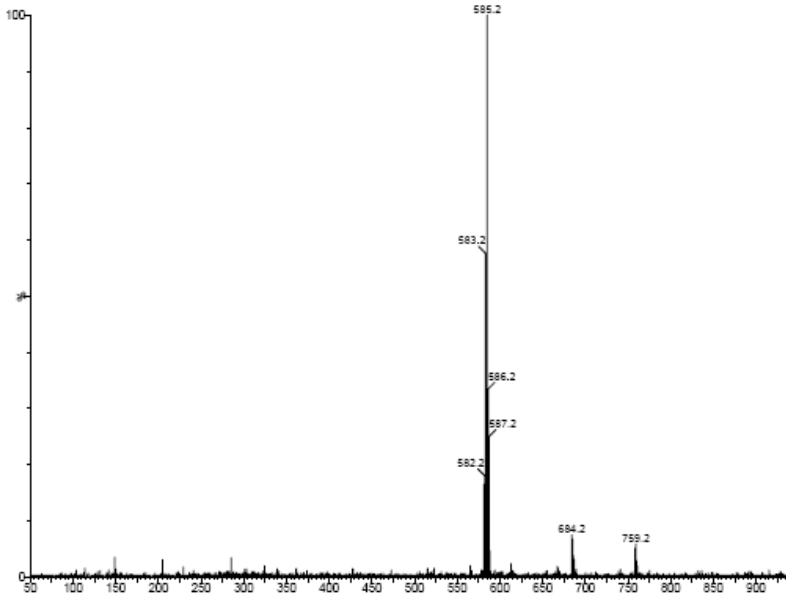

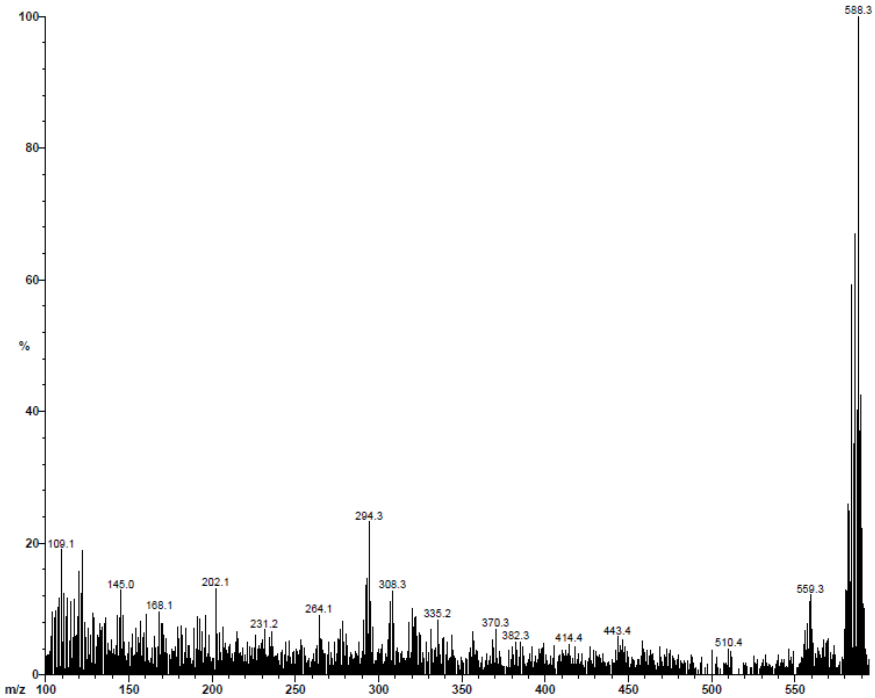

Figure S148. ESI (top) and electron impact mass spectra of phenyl benzoselenacarbaporphyrin **15d**.

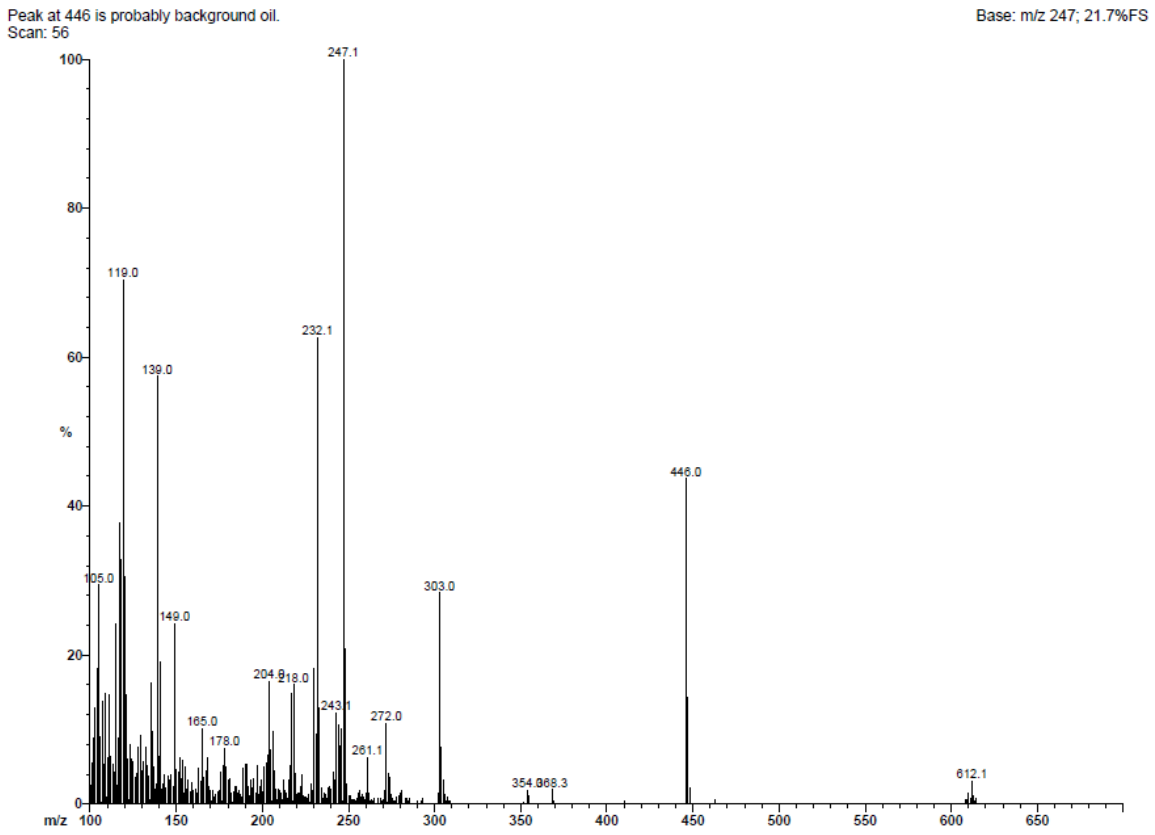

Figure S149. ESI (top) and electron impact mass spectra of phenyl benzoselenacarbaporphyrin aldehyde **16d**.

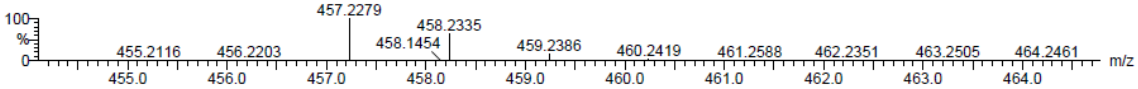

Minimum:				-1.5		
Maximum:		5.0	10.0	600.0		
Mass	Calc. Mass	mDa	PPM	DBE	i-FIT	Formula
457.2279	457.2280	-0.1	-0.2	19.5	84.7	C32 H29 N2 O
	457.2240	3.9	8.5	15.5	120.4	C27 H29 N4 O3

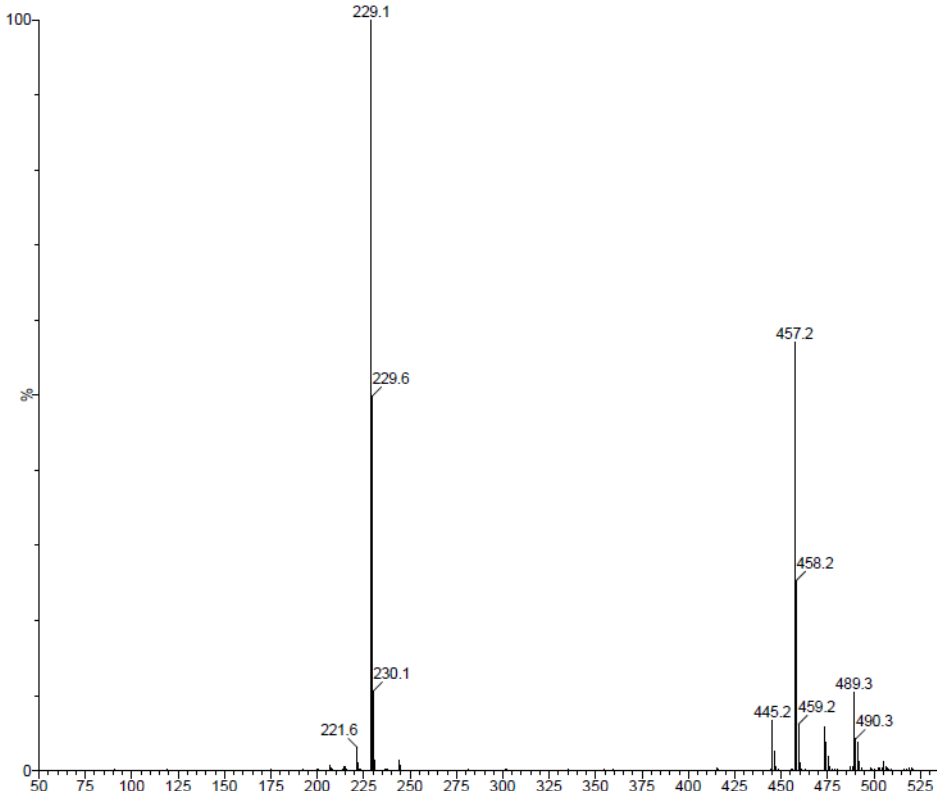

Figure S150. Electrospray ionization mass spectrum of oxa-azuliporphyrin **12a**.

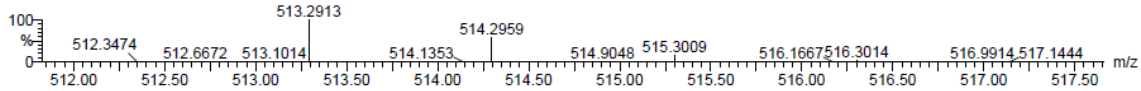

Minimum:				-1.5		
Maximum:		5.0	10.0	600.0		
Mass	Calc. Mass	mDa	PPM	DBE	i-FIT	Formula
513.2913	513.2906	0.7	1.4	19.5	58.4	C36 H37 N2 O
	513.2866	4.7	9.2	15.5	99.8	C31 H37 N4 O3

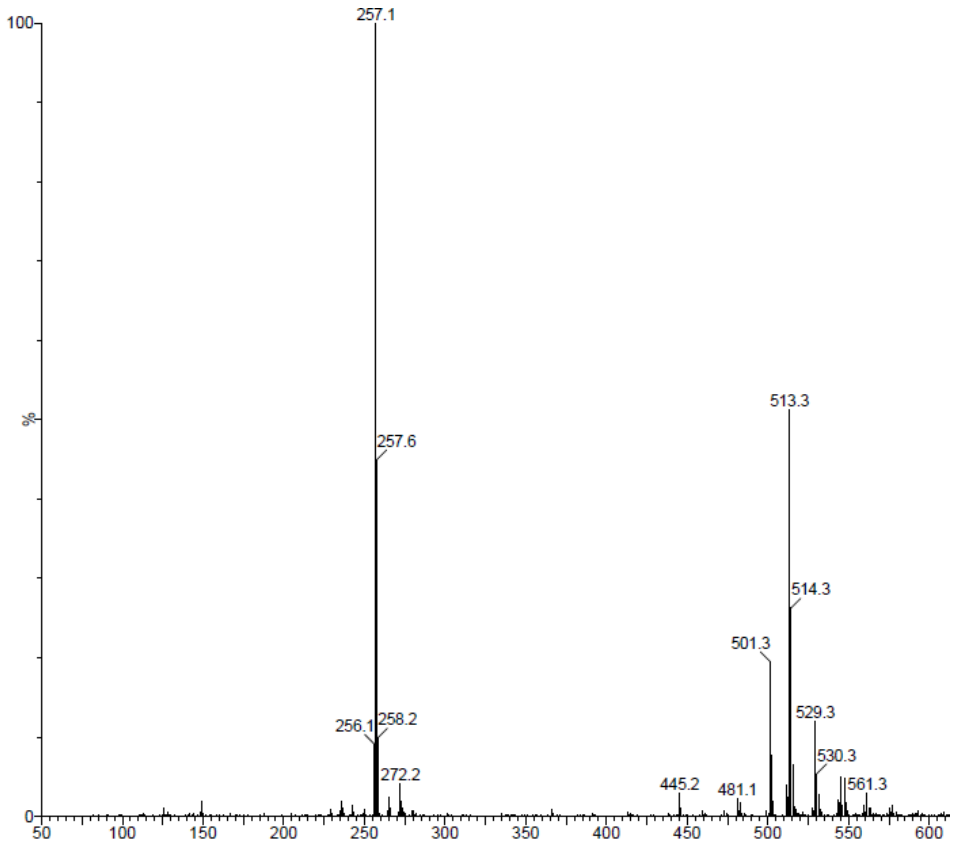

Figure S151. Electrospray ionization mass spectrum of *tert*-butyl oxa-azuliporphyrin **12b**.

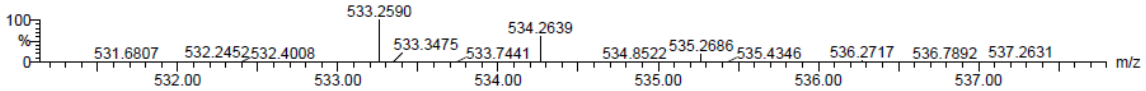

Minimum:				-1.5		
Maximum:		5.0	10.0	600.0		
Mass	Calc. Mass	mDa	PPM	DBE	i-FIT	Formula
533.2590	533.2593	-0.3	-0.6	23.5	65.9	C38 H33 N2 O
	533.2553	3.7	6.9	19.5	105.3	C33 H33 N4 O3

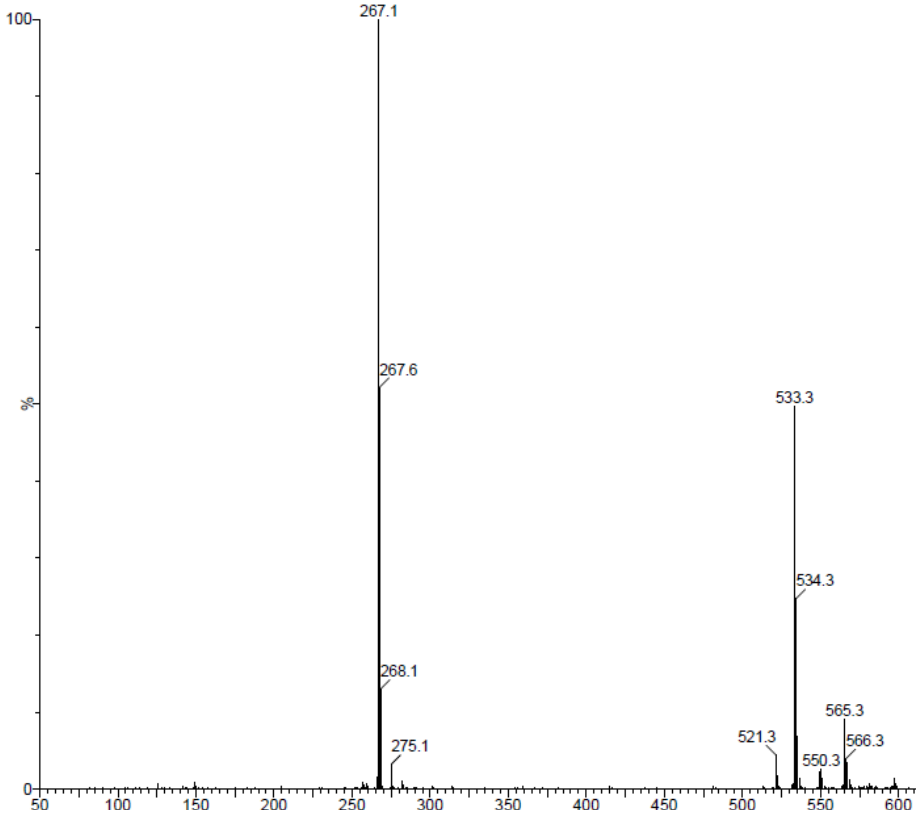

Figure S152. Electrospray ionization mass spectrum of phenyl oxa-azuliporphyrin **12c**.